◆ Human Brain Mapping 37:1661–1683 (2016) ◆

Intracranial EEG Potentials Estimated From MEG Sources: A New Approach To Correlate MEG and iEEG Data in Epilepsy

Christophe Grova,[1,2,3,4]* Maria Aiguabella,[1] Rina Zelmann,[1] Jean-Marc Lina,[4,5,6] Jeffery A. Hall,[1] and Eliane Kobayashi[1]

[1]Montreal Neurological Institute, Department of Neurology and Neurosurgery, McGill University, Montreal, Québec, Canada
[2]Multimodal Functional Imaging Lab, Biomedical Engineering Department, McGill University, Montreal, Québec, Canada
[3]Physics Department and PERFORM Centre, Concordia University, Montreal, Québec, Canada
[4]Centre De Recherches En Mathématiques, Montreal, Québec, Canada
[5]Electrical Engineering Department, Ecole De Technologie Supérieure, Montreal, Québec, Canada
[6]Centre D'etudes Avancées En Médecine Du Sommeil, Centre De Recherche De L'hôpital Sacré-Coeur De Montréal, Montreal, Québec, Canada

Abstract: Detection of epileptic spikes in MagnetoEncephaloGraphy (MEG) requires synchronized neuronal activity over a minimum of 4cm2. We previously validated the Maximum Entropy on the Mean (MEM) as a source localization able to recover the spatial extent of the epileptic spike generators. The purpose of this study was to evaluate quantitatively, using intracranial EEG (iEEG), the spatial extent recovered from MEG sources by estimating iEEG potentials generated by these MEG sources. We evaluated five patients with focal epilepsy who had a pre-operative MEG acquisition and iEEG with MRI-compatible electrodes. Individual MEG epileptic spikes were localized along the cortical surface segmented from a pre-operative MRI, which was co-registered with the MRI obtained with iEEG electrodes in place for identification of iEEG contacts. An iEEG forward model estimated the influence of every dipolar source of the cortical surface on each iEEG contact. This iEEG forward model was applied to MEG sources to estimate iEEG potentials that would have been generated by these sources. MEG-estimated iEEG potentials were compared with measured iEEG potentials using four source localization methods: two variants of MEM and two standard methods equivalent to minimum norm

Additional Supporting Information may be found in the online version of this article.

Contract grant sponsors: Canadian Institutes of Health Research MOP 93614 (EK), Montreal Neurological Institute-Centre of Excellence in Commercialization and Research Grant (EK), Natural Sciences and Engineering Research Council of Canada Discovery Grant Program and Discovery Accelerator Supplement award (CG), Fonds de Recherche en Santé du Québec (FRSQ; to C.G.), and American Epilepsy Society Early Career Physician-Scientist award and FRSQ (to E.K.).

*Correspondence to: Christophe Grova, PhD; Assistant Professor, Physics Department, PERFORM Centre, Concordia University, Loyola Campus – Office SP 365.12, 7141 Sherbrooke Street West, Montreal, QC H4B 1R6, Canada. E-mail: christophe.grova@concordia.ca

Christophe Grova and Maria Aiguabella contributed equally to this manuscript.

Received for publication 31 July 2015; Revised 18 December 2015; Accepted 17 January 2016.

DOI: 10.1002/hbm.23127

Published online 2 March 2016 in Wiley Online Library (wileyonlinelibrary.com).

and LORETA estimates. Our results demonstrated an excellent MEG/iEEG correspondence in the presumed focus for four out of five patients. In one patient, the deep generator identified in iEEG could not be localized in MEG. MEG-estimated iEEG potentials is a promising method to evaluate which MEG sources could be retrieved and validated with iEEG data, providing accurate results especially when applied to MEM localizations. *Hum Brain Mapp 37:1661–1683, 2016.*

Key words: epilepsy; neurophysiology; epileptic spikes; magnetic source imaging; magnetic resonance imaging; source localization; intracranial EEG; epilepsy surgery; presurgical investigation

INTRODUCTION

Epilepsy is a chronic disorder that affects up to 1% of the population worldwide, in which up to 40% of patients are refractory despite multiple antiepileptic drugs [Kwan and Brodie, 2000]. Surgery can be envisaged for many of these patients, but the challenge that impacts surgical decision is to accurately localize the epileptic focus. Scalp monitoring of video-electroencephalography (EEG) and a good quality magnetic resonance imaging (MRI) scans are the first non-invasive tests performed in any pre-surgical work-up. They can localize the focus suspected by clinical semiology in many but not all patients. Additional non-invasive techniques such as ictal/interictal single photon emission computed tomography (SPECT) [Kim and Mountz, 2011], positron emission tomography (PET) [Juhasz and Chugani, 2003], functional MRI (fMRI) [An et al., 2013; Gotman, 2008] and magnetoencephalography (MEG) [Knowlton et al., 2006; Sutherling et al., 2008] are also utilized in each individual patient, depending on each epilepsy center protocol [Duncan, 2010; Knowlton et al., 2008; Theodore, 1989].

Despite all these available non-invasive explorations, we are often urged to proceed with invasive investigation using intracranial EEG recordings. Intracranial EEG allows a tunnelled but yet precise evaluation at millimetric resolution of targeted brain regions, either acutely through intraoperative electrocorticography or chronically through intracranial depth electrodes/subdural grids recordings. Intracranial EEG is the gold standard technique to confirm the location of the seizure focus, but it relies on a priori hypothesis of the topography of the epileptogenic zone as well as its associated epileptogenic network [Chauvel et al., 1996]. The limited spatial sampling requires an optimal implantation strategy to which results of non-invasive techniques contribute complementarily. Correct targeting determines the yield and risks of intracranial EEG.

MEG is complementary to other standard non-invasive investigations [Knake et al., 2006; Pataraia et al., 2004] and also to intracranial EEG [Agirre-Arrizubieta et al., 2009; Knowlton et al., 2006; Knowlton et al., 1997; Mikuni et al., 1997; Minassian et al., 1999; Shigeto et al., 2002; Stefan et al., 1992; Sutherling et al., 1988]. Interictal epileptic activity is commonly used as an epilepsy neurophysiological biomarker for each patient [Noachtar and Remi, 2009]. It allows diagnosis and classification of the epilepsy syndrome. Visual identification of these abnormal paroxysms (e.g. epileptic spikes) from signals recorded non-invasively from the scalp requires that their generators in the cortex have a minimum spatial extent [Ebersole, 1997; Huiskamp et al., 2010; Mikuni et al., 1997; Oishi et al., 2002; Tao et al., 2007]. One of the main advantages of using MEG over EEG is increased spatial accuracy, since, contrary to EEG, MEG data are not spatially smeared by the poorly conductive skull [Hamalainen et al., 1993]. Studies comparing scalp and intracranial recordings reported that epileptic spikes to be detected in scalp recordings, require generators to be extended within 4cm^2 of cortex in MEG [Mikuni et al., 1997; Oishi et al., 2002; Shigeto et al., 2002]. Regional differences have also been reported with some cortical areas resulting mainly in tangential dipolar sources (e.g., occipital pole, temporal plane, post-central sulcus, orbitofrontal region) and more likely to generate large MEG signals [Huiskamp et al., 2010]. A minimum area of 10 cm^2 was suggested in EEG by Tao et al. [2007] using simultaneous acquisition of scalp EEG with intracortical grids. Using biophysical and neurophysiological modeling, Cosandier-Rimélé et al. confirmed that a cortical surface ranging from 18 to 20 cm^2 should be involved to generate a typical neocortical temporal lobe epileptic spike measured in intracranial EEG and scalp EEG [Cosandier-Rimélé et al., 2007; Cosandier-Rimélé et al., 2008]. The findings reported by Tao et al. [2007] have been carefully validated using extensive realistic simulations using a finite element model of the head [von Ellenrieder et al., 2014], in which the correspondance between the actual extent along the cortical surface versus the number of electrodes involved in intra-cortical grid has been studied.

Source localization of MEG epileptic spikes has been mainly performed by modeling brain activity with few equivalent current dipole (ECD) sources [Knowlton et al., 2006; Leijten et al., 2003; Mikuni et al., 1997; Oishi et al., 2002; Papanicolaou et al., 2005; Schwartz et al., 2003; Wennberg and Cheyne, 2014]. Whereas this is the only clinically approved method, ECD can localize at best the center of mass of these spatially extended generators [Ebersole, 1997]. ECD localization can often be misleading in presence of large spatially extended generators, resulting in false deep localizations [Kobayashi et al., 2005]. Dipole scanning approaches using spatial filters, sequentially assessing the contribution to the data of any dipolar source on a 3D grid within the brain,

have also been proposed [Agirre-Arrizubieta et al., 2009; Bouet et al., 2012; Ishii et al., 2008]. It has never been carefully demonstrated through numerical simulations that dipole scanning approaches could be sensitive to the spatial extent of the sources, except by replacing the local single dipole model by a realistically shaped extended source along the cortical surface [Birot et al., 2011; Hillebrand and Barnes, 2011]. However, correlation between the spatial extent of source localization obtained using a standard Beamformer estimated on a 3D grid and intracranial iEEG with implanted depth electrodes has been suggested [Bouet et al., 2012; Jung et al., 2013]. In this context, incorporation of realistic anatomical constraints by estimating source activity distributed along the cortical surface [Dale and Sereno, 1993] is an interesting option to recover the spatial extent of the sources. Standard distributed sources methods like the Minimum Norm Estimate (MNE) [Hämäläinen and Ilmoniemi, 1994] are very popular and can accurately describe the location and time course of epileptic source activity, as well as its propagation patterns [Tanaka et al., 2010]. However, the ability of MNE to recover the spatial extent of the generators is questionable [Ding, 2009].

We previously proposed the Maximum Entropy on the Mean (MEM) regularization framework [Amblard et al., 2004], a new source localization method, which demonstrated its ability to localize accurately the generators of epileptic activity together with their spatial extent. When compared to other distributed methods, MEM demonstrated excellent performance to recover spatially extended sources when applied on realistic simulations of epileptic spikes either in EEG [Grova et al., 2006] and or in MEG [Chowdhury et al., 2013; Lina et al., 2014]. MEM also suggested promising results when applied on clinical data. We found good spatial correspondence between the extent of MEM sources and hemodynamic responses to similar epileptic discharges recorded using simultaneous EEG/fMRI [Grova et al., 2008; Heers et al., 2014]. In a recent study, MEM showed a positive predictive value of 0.79, where the maximum amplitude of MEM sources was qualitatively validated with intracranial EEG data for 14 out of 19 patients [Heers et al., 2016].

Whereas realistic simulations offer a well-controlled framework to validate and to compare source localization methods [Birot et al., 2011; Chowdhury et al., 2013; Grova et al., 2006], clinical evaluation involving clinical data is more difficult and has been mainly addressed using invasive recordings. In this paper, we will refer to ECoG for intracranial recordings using subdural grids and to iEEG for intracranial recordings using implanted depth electrodes. Most validation studies in MEG were based on comparison with ECoG recordings [Agirre-Arrizubieta et al., 2009; de Gooijer-van de Groep et al., 2013; Fujiwara et al., 2012; Knowlton et al., 2006; Leijten et al., 2003; Mikuni et al., 1997; Minassian et al., 1999; Oishi et al., 2002; Tanaka et al., 2010]. Fewer studies have compared MEG sources with iEEG recordings [Badier et al., 2016; Bouet et al., 2012; Gavaret et al., 2014; Heers et al., 2016; Jung et al., 2013; Schwartz et al., 2003]. As ECoG is performed with subdural contacts, evidently this technique allows recording of the most superficial aspects of the cortex only, whereas iEEG with depth electrodes records from superficial neocortical and deeper structures such as the bottom of the sulci [Chauvel et al., 1996; Olivier et al., 1994]. Validation of EEG/MEG source localization with ECoG and iEEG recordings is only feasible and valid for the near vicinity of implanted brain regions [Merlet and Gotman, 2001]. Consequently, ECoG or iEEG have been mainly used to infer sublobar accuracy of source localization results [Agirre-Arrizubieta et al., 2009; Bouet et al., 2012; de Gooijer-van de Groep et al., 2013; Fujiwara et al., 2012; Heers et al., 2016; Jung et al., 2013; Knowlton et al., 2006; Leijten et al., 2003; Mikuni et al., 1997; Minassian et al., 1999; Oishi et al., 2002; Schwartz et al., 2003; Tanaka et al., 2010]. In order to provide accurate quantitative analysis, one should take into account the distance between MEG sources and iEEG electrode contacts. Moreover, comparing MEG at the source level and iEEG at the signal level consists in comparing information of different natures, i.e., current density in A.m versus electrical potentials in V. ECoG source localization has been proposed to address this issue, converting local electrical potentials into current density distributions [Cho et al., 2011; Dumpelmann et al., 2009; Fuchs et al., 2007; Ramantani et al., 2013; Zhang et al., 2008]. To the best of our knowledge, just one simulation study [Chang et al., 2005] addressed the difficult problem of iEEG source localization. Another approach consists in estimating directly cortical electrical potentials from scalp EEG data [Gevins et al., 1994; Grave de Peralta Menendez et al., 2000; He et al., 2002], however such strategies have not been adapted neither for MEG data nor for iEEG data with depth electrodes.

The objective of the present study is to propose a new method to evaluate spatio-temporal correlations between MEG sources and iEEG findings at the time of epileptic discharges. Alternatively to attempt to solve the difficult problem of iEEG source localization, here we propose to convert MEG sources localized along the cortical surface into estimated iEEG potentials. These MEG-estimated iEEG potentials could then be directly compared with recorded iEEG potentials. This conversion is achieved using accurate localization of the depth electrodes with respect to the underlying anatomy and by then applying an iEEG forward model to MEG sources. This method, allowing a new way to further understand the link between MEG and iEEG recordings, is illustrated on five clinical cases of focal epilepsy patients. For each patient, results obtained using two MEM-based localization approaches were compared with two standard distributed sources methods.

MATERIALS AND METHODS

Ethics

This study was conducted in compliance with the Code of Ethics of the World Medical Association (Declaration of

Helsinki), the standards established by the Montreal Neurological Institute Research Ethics Board and the standards of our granting agencies.

Patients

All patients signed informed consents for participation in the study, approved by our institution Research Ethics Board, in which the nature of the experimental procedures was clearly explained. We retrospectively selected from our MEG database patients with extra-temporal drug-resistant focal epilepsy who had spikes during the MEG recording and later underwent iEEG with MRI-compatible electrodes. Our recruitment consisted in consecutive patients recruited in 2011-2013, who participate to our usual EEG/MEG investigation and were then implanted with MR-compatible electrodes. According to these criteria, five patients were included with the following epileptic foci: right orbitofrontal (N = 3), right frontal SMA-cingulate gyrus (N = 1) and right inferior frontal (N = 1). MRI findings were: normal (N = 1), suspected for an underlying focal cortical dysplasia (FCD, N = 3) and hemimegalencephaly (N = 1).

MEG Acquisition

Acquisitions were performed at the MEG Center at University of Montreal, using a CTF scanner (VSM MedTech - CTF Systems Inc - Vancouver), equipped with 275 axial gradiometers. Simultaneous EEG was recorded with 56 electrodes cap (10-10 system) with the nose as recording reference. Additional electrodes for electrocardiogram monitoring and electrooculogram were applied. Sampling rates for EEG/MEG acquisitions were 1200 Hz. MEG sensor positions were monitored during the whole acquisition using continuous head localization, with localization coils placed over three fiducial points (i.e., nasion, right and left pre-auricular points). To minimize head movements, all recordings were done with subjects lying supine on a bed. Scanning sessions aimed at 10 runs of six minutes recording at rest, constrained by the cooperation and tolerance from each patient. Medications were not changed for the purpose of recording.

iEEG Acquisition

iEEG investigation using intracranial MRI-compatible depth electrodes (Dixi medical, Besancon, France) was planned based on information obtained during standard clinical investigation (derived from scalp video-EEG recordings, clinical MRI, PET and neuropsychology evaluation). Decision for the number of electrodes and their location was taken by the neurophysiologist and the neurosurgeon. MEG results were made available, and their relevance for electrode targeting was subject to the discretion of the physicians. Electrodes consisted in D08 electrodes from Dixi Medical (Besançon, France), made with platine iridium to allow MR compatibility, 0.8 mm diameter. Depending on the regions targeted, electrodes composed with either 10 or 14 contacts were implanted. Along the electrode, the length of every contact was 2mm, with 1.5mm distance between contacts. Depth electrodes were implanted stereotactically using an image-guidance system (SNN Neuronavigation System, Mississauga, Canada) [Olivier et al., 1994]. iEEG signals were recorded at 2000Hz sampling rate, using Harmonie monitoring system (Stellate, Montreal, Canada) until enough ictal and interictal information was obtained for each patient (6 to 16 days).

MRI Acquisitions

High-resolution preoperative anatomical T1 1mm isotropic 3D acquisition (MPRAGE: 192 sagittal slices, 1 mm slice thickness, 256x256 matrix, TE = 2.98 ms, TR = 2.3 s, flip angle 9°) was obtained in the 3T scanner (Siemens, Tim Trio) for modelling the anatomy of the subject and extraction of the cortical surface. A post-implantation T1-weighted anatomical MRI was acquired in the 1.5T scanner (GE Medical Systems, Signa Excite), allowing visualization of electrodes through the void artifact in the images. This second scan was performed between days 2-4 post-implantation (180 sagittal slices, 1 mm slice thickness, 512x512 matrix, TE = 8 ms, TR = 23 ms, flip angle 20°).

MRI and MEG Preprocessing

The 3T MRI was used to model the anatomy for MEG source localization. This requires first an accurate MRI/MEG co-registration, using the position of three localization coils over fiducial points and that of multiple points sampled over the scalp, nose and peri-ocular regions (called 'headshape') digitized using a Polhemus Isotrak system prior the MEG recording session. Location of the fiducial points on the MRI was used to compute a first rigid transformation matrix (3 rotations, 3 translations). The co-registration accuracy was further optimized by fitting the headshape to the skin surface, segmented from the MRI. The next step comprised a realistic modeling of each subject's anatomy. To model the source space, the cortical surface consisting in the grey/white matters interface was segmented from the MRI of each subject [Mangin et al., 1995], using BrainVISA-4.2.1 software (http://www.brainvisa.info). The resulting distributed sources model consisted in a realistic 3D mesh of the cortical surface (sub-sampled to 8000 vertices, inter-node distance: 3mm) with each dipolar source oriented perpendicular to the local cortical surface.

Solving the inverse problem for MEG source localization first relies on an accurate solution of the forward model. The forward model estimates, for any known dipolar source within the brain, its contribution to signals

captured in all MEG sensors. We used the Boundary Element Method (BEM) to compute the forward model. A one-layer BEM model using the inner skull surface was estimated using the implementation of OpenMEEG [Gramfort et al., 2011; Kybic et al., 2006] within Brainstorm software [Tadel et al., 2011] (http://neuroimage.usc.edu/brainstorm/). The inner skull surface was segmented from the anatomical MRI of each subject using Brainstorm software. A homogeneous conductivity of $\sigma = 0.33$ S.m^{-1} within the brain was assumed [Goncalves et al., 2003; Hamalainen et al., 1993].

MEG Epileptic Spike Marking

MEG epileptic spikes were marked in DataEditor signal browser (CTF), using 0.3-70Hz band pass filtered signals. Individual MEG spikes were visually identified and marked at their maximum peak by a neurophysiologist and those spikes with good inter-rater agreement were kept for analysis. Epileptic discharges coinciding with EKG peaks were discarded. MEG epileptic spikes were classified according to their spatial distribution and similar spikes were considered for source localization. We did not constrain the maximum or minimum number of epileptic spikes marked per patient, as the spiking rate varied amongst them.

MEG Source Localization

Using anatomical constraints [Dale and Sereno, 1993], the relationship between source amplitudes and MEG measurements is expressed by the following linear model:

$$M = G\ J + E \tag{1}$$

where M is a $q \times \tau$ matrix of the MEG signal measured at $q=275$ MEG sensors and τ time samples. E models an additive measurement noise ($q \times \tau$ matrix). J is a $p \times \tau$ unknown matrix of the current density along the cortical surface ($p \cong 8000$ unknown dipolar moment amplitudes of sources oriented normally to the cortical surface). G indicates the $q \times p$ lead field matrix obtained by solving the MEG forward problem estimating the contribution of each dipolar source on each MEG sensor.

MEG epileptic spikes were localized using MEM localization method [Chowdhury et al., 2013; Grova et al., 2006]. The key concept of the MEM approach, originally proposed in Amblard et al. [2004] is the assumption that brain activity can be characterized by K cortical parcels along the cortical surface [Lapalme et al., 2006]. MEM inference is able to specifically switch these parcels *on* or *off* and to estimate a contrast of source intensities within the selected active parcels. The number of parcels may vary between few dozens to few hundreds. Here, we used a number of parcels of similar order as the number of MEG sensors ($K \cong 200$ parcels). These properties allow MEM to localize and to determine the spatial extent of the epileptic spike generators along the cortical surface [see Chowdhury et al., 2013 and Grova et al., 2006 and Supporting Information, Figure S1 for further details and evaluation].

In the MEM framework, we consider the amplitude of the sources J to be estimated as a multivariate random variable with a probability distribution $dp(j) = Prob(J=j)\ dj$. Assuming a collection of K mutually independent parcels, we proposed the following reference distribution $d\nu$ to model our knowledge of the current density distribution:

$$d\nu(j) = \prod_{k=1}^{K} [(1-\alpha_k)\ \delta(j_k) + \alpha_k\ \mathcal{N}(\mu_k,\ \Sigma_k)]\ dj_k \tag{2}$$

where α_k denotes the probability of the k^{th} parcel to be active. Multivariate j_k denotes the intensities of the p_k sources in the k^{th} parcel. δ refers to the Dirac distribution allowing to "shut down" inactive parcels ($\alpha_k=0$). $\mathcal{N}(\mu_k,\ \Sigma_k)$ is a Gaussian distribution describing the intensities of the k^{th} parcel when active ($\alpha_k=1$), where μ_k and Σ_k represent, respectively, the mean and the covariance of the p_k sources within the k^{th} parcel.

Regularization within the MEM framework is obtained by writing the solution dp in the form of $dp(j)=f(j)\ d\nu(j)$, where the reference distribution $d\nu(j)$ as defined by Eq. (2) expresses a prior model on the sources J and $f(j)$ is a ν- density to be found such that it explains the data in average:

$$M = \mathbb{E}_{dp}[G\ j] = \int G\ j\ f(j)\ d\nu(j) \tag{3}$$

where $\mathbb{E}_{dp}$ denotes the expectation (average) according to the distribution dp. Among all the distributions dp satisfying the above constraint (i.e., ensuring data fit), the MEM solution $d\hat{p}(j)=\hat{f}(j)\ d\nu(j)$ is the one with maximum ν -entropy. The resulting current density distribution $\hat{J}_{MEM}$ estimated using MEM regularization is then obtained as the first moment (or expectation) of the distribution $d\hat{p}$ (i.e., $\hat{J}_{MEM} = \mathbb{E}_{d\hat{p}}[j]$) . The probability of every parcel to be active (α_k) was initialized using the Multivariate Source Prelocalization [Mattout et al., 2005], a projection method estimating a coefficient, which characterizes the contribution of each dipolar source to the data. Two variants of the MEM technique were investigated:

- MEM source localization, where the mean of every active parcel μ_k was initialized as 0 and Σ_k as a diagonal matrix (Minimum Norm assumption).
- Coherent MEM (cMEM) source localization, where the mean of every active parcel μ_k was initialized as 0 and Σ_k was initialized using diffusion-based spatial priors [Harrison et al., 2007], modeling local spatial smoothness along the cortical surface within each parcel (maximum local spatial smoothness assumption).

The implementation of MEM and cMEM methods evaluated in this study is available within the Brain Entropy in Space and Time (Best) toolbox that we recently released as a plug-in in Brainstorm software: http://neuroimage.usc.edu/brainstorm/Tutorials/TutBEst

As a continuation of the clinical study of Heers et al. [2016], in which we assessed sublobar regional accuracy between EEG sources, MEG sources, and iEEG data, we considered the same source localization methods in this quantitative evaluation study. Therefore, MEM and cMEM were compared with two standard source localization methods, implemented within the Restricted Maximum Likelihood (ReML) framework to estimate regularization hyperparameters [Friston et al., 2002]:

- Independent and Identically Distributed (IID) model: This method assumes source covariance to be modeled as an identity matrix, providing a minimum energy solution, similar to the one originally proposed by Hämäläinen and Ilmoniemi [1994].
- Spatially Coherent Sources (COH): This method assumes source covariance to be modeled as a linear combination of an identity matrix (minimum norm prior) and a diffusion-based spatial prior imposing spatial smoothness along the cortical surface [Harrison et al., 2007]. This method provides a solution that is spatially smooth, equivalent to LORETA originally proposed by Pascual-Marqui et al. [1994].

Source localization using MEM, cMEM, IID, and COH was applied to every single MEG epileptic spike.

iEEG Signal Processing

Although patients had seizures recorded during iEEG investigation, for our study, we only analyzed interictal iEEG epileptic spikes. iEEG spikes were visually identified using a bipolar or monopolar montage in band-pass filtered signals (0.3–70 Hz). Epileptic spikes were marked at their maximum peak, classified based on the anatomical location and contacts distribution. Following a similar strategy, we already considered when comparing EEG/fMRI to iEEG data [Benar et al., 2006; Daunizeau et al., 2007; Grova et al., 2008], one key criterion was to select iEEG discharges with clear involvement of the most superficial iEEG contacts, most likely to generate signals visually detectable on the scalp, using either EEG or MEG. For patients showing clear, large amplitude and highly reproducible typical epileptic spikes, with excellent signal-to-noise ratio in both iEEG and MEG, involving superficial iEEG contacts, only few discharges were selected (around 5–10) to provide a reliable picture of the iEEG/MEG correspondance (e.g., Patients 1 and 2). For other patients with more complex recordings (e.g., Patients 3 and 4) and small amplitude MEG discharges (Patient 5), all possible epileptic spikes fulfilling our criteria (typical of the epilepsy for each patient and with involvement of superficial iEEG contacts) selected within a 1 h recording were therefore considered for the analysis.

Quantitative Analysis of Concordance between MEG Sources and iEEG Findings

- Accurate localization of iEEG electrodes: iEEG contacts locations were derived from the MRI obtained with electrodes in place and from the technical information/specifications from each electrode implanted (steps summarized in Fig. 1). Electrodes positions were manually drawn by (1) marking the void artefact produced by the electrodes and contacts in the brain volume, using Display software[1]; (2) identification of a connecting line in the void artefact between the entry point (most superficial) and the target point (deepest) for each electrode; (3) estimation of the exact location of each recording contact along this line using the actual distance between contacts (3.5 mm as per manufacturer specifications); and (4) 3D representation of each contact using the mesh of a sphere (with a 2 mm diameter as specified by manufacturer) centered at each contact location computed within BrainVISA environment. To ensure spatial accuracy between MEG sources along the cortical surface and iEEG electrodes, the high-resolution preimplantation 3T MRI was coregistered with the postimplantation 1.5 T MRI with electrodes in place. MRI-to-MRI registration was performed using Animal software [Collins et al., 1994], by maximizing the correlation coefficient between the two volumes using a rigid transformation (3 translations, 3 rotations, and 1 scaling parameter).
- Converting MEG sources into simulated iEEG signals: To assess what part of MEG sources estimated along the cortical surface could be detected by every iEEG contact, we used an estimation of the iEEG forward model G_{iEEG} to assess the contribution of every dipolar source along the cortical source to every iEEG contact. G_{iEEG} is an $n \times p$ matrix estimating, for each equivalent current dipole of unit activity $\vec{j}_i$ located on the vertex S_i and oriented along $\vec{n}_i$ the normal to the cortical surface ($i=1,\ldots,p$), the corresponding electrical potential V at the j^{th} iEEG electrode contact located at $E_j (j=1,\ldots,n)$. Assuming an infinite volume conductor characterized by its conductivity σ, the electrical potential is computed as

$$V(E_j) = \frac{\vec{n}_i \cdot \vec{u}_r}{4 \pi \sigma r^2} \quad (4)$$

where $\vec{u}_r$ is a unit vector oriented from the source point S_i to the measurement point E_j , and r is the

[1]Display software: http://www.bic.mni.mcgill.ca/ServicesSoftwareVisualization/

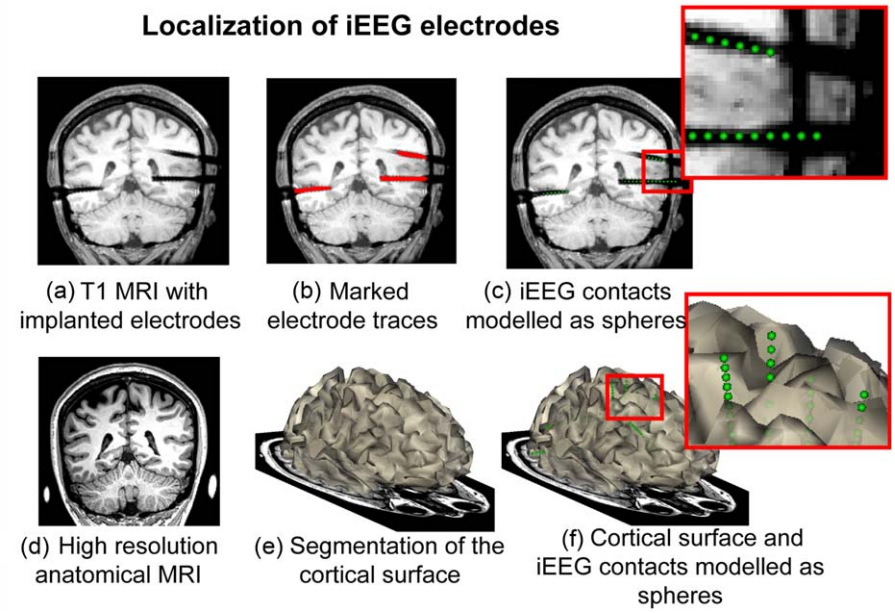

Figure 1.

Localization of iEEG electrodes contacts on the high-resolution MRI used for MEG source localization. The preimplantation 3 T MRI (**d**) and the postimplantation 1.5 T MRI obtained with MR-compatible iEEG electrodes (**a**) were used for accurate location of iEEG recording contacts. First, void artefacts from electrodes tracks were marked over the 3D volume of the postimplantation MRI (**b**). Second, the entry point and the target point for each electrode were determined to provide a nondistorted connecting line, along which the recording contacts were placed, based on the manufacturer's specifications of intercontacts distance and contacts dimensions. Every iEEG electrode contact was modeled as a sphere (**c**). Finally, the two MRI volumes were coregistered and iEEG electrodes contacts were represented over cortical surface segmented from the high-resolution preimplantation volume (**f**). [Color figure can be viewed in the online issue, which is available at wileyonlinelibrary.com.]

Euclidean distance between S_i and E_j. Comparing the infinite volume conductor model with a three-shell spherical model to estimate G_{iEEG}, Cosandier-Rimélé et al. [2007] showed that infinite volume conductor model tended to slightly underestimate the electrical potential. Choosing a lower conductivity σ of 0.25 $\mathrm{S \cdot m^{-1}}$ instead of 0.33 $\mathrm{S \cdot m^{-1}}$, they showed that very realistic simulated iEEG epileptic signals, mimicking almost perfectly real iEEG measurements, could be obtained by both models. It is important to mention that Eq. (4) is valid only if the measurement E_j is performed at a certain distance from the source, otherwise the dipolar assumption does not hold anymore. Using finite-element models, von Ellenrieder et al. [2012] demonstrated that when modeling the impact of the shape of the iEEG electrode on local electrical potentials, no significant impact was observed at a distance of 2 mm from the electrode. Assuming an iEEG-MRI coregistration accuracy of 3 mm, as suggested using a registration approach similar to ours [Dykstra et al., 2012], we proposed the following model to prevent instabilities of the model caused by too close measurements:

$$V(E_j) = \frac{\vec{n_i} \cdot \vec{u_r}}{4\ \pi\ \sigma\ r^2} \text{ if } r > r_0 = 3\ mm \text{ and}$$
$$V(E_j) = \frac{\vec{n_i} \cdot \vec{u_r}}{4\ \pi\ \sigma\ {r_0}^2} \text{ if } r \leq r_0 = 3\ mm \quad (5)$$

Only iEEG electrodes located inside the inner skull surface, at more than 2 mm from the surface, were selected for this analysis. The iEEG forward model was finally applied to the current density along the cortical surface $\hat{J}_{MEG}$ obtained from MEG source localization, thus estimating the resulting iEEG electrical potentials that would have been generated by MEG sources:

$$V_{MEG} = G_{iEEG}\ \hat{J}_{MEG} \quad (6)$$

- For each epileptic spike marked in MEG, MEG source localization was performed (using MEM, cMEM, IID, and COH) and corresponding V_{MEG} potentials were computed. MEG/iEEG comparison was performed by representing the time courses of the actual recorded V_{iEEG} potentials with the estimated V_{MEG} potentials on all iEEG contacts. In both cases, we present the

average electrical potential obtained over all epileptic spikes ± standard deviation estimated from all individual spikes. Since it is expected that MEG source localization would underestimate the actual current density, only relative amplitudes of V_{MEG} and V_{iEEG} were compared, by normalizing each of them by the maximum potential obtained on the averaged epileptic spike. Spatially, the absolute value of MEG sources shown as a color texture mapped along the cortical surface were represented together with the absolute value of recorded V_{iEEG} potentials and estimated V_{MEG} potentials mapped as a color texture on the iEEG contacts, at the peak of the average epileptic spike. Illustrations of combined MEG sources over the cortical surface, V_{iEEG} and V_{MEG} results over electrode contacts modeled as spheres and high-resolution preimplantation MRI were generated using Anatomist software[2].

- Quantitative comparison between V_{MEG} and V_{iEEG}: four complementary comparison metrics were proposed to quantify the correspondance between the estimated V_{MEG} and measured V_{iEEG} potentials. Each metric was computed taking into account V_{iEEG} potentials at the peak of the average iEEG epileptic spike and the estimated V_{MEG} potentials, for five time samples around the peak of the average MEG spike. The average metric obtained from these five estimates was finally reported. We first computed the spatial correlation coefficient (Corr) between V_{iEEG} potentials at the peak of the average iEEG epileptic spike and the estimated V_{MEG} potentials, in five time samples around the peak of the average MEG spike. We also reported the minimum Euclidean distance (D_{min}) between the contact showing the maximum absolute amplitude in V_{iEEG} with the contact showing the maximum absolute amplitude in V_{MEG} for the same time points. We then considered a measure of spatial dispersion (SD) [Molins et al., 2008] between the contacts showing maximum activity in V_{iEEG} and the spatial distribution of average estimated V_{MEG} potentials. Following a strategy we already considered for our previous study [Heers et al., 2016], SD metric was measured as follows:

$$SD = \sqrt{\frac{\sum_{i=1}^{n}\left(min_{j\in\Theta}(D_{ij})\ V_{MEG,i}^{2}\right)}{\sum_{i=1}^{n}V_{MEG,i}^{2}}} \qquad (7)$$

where Θ denotes the reference set of contacts considered as the true spatial extent of the spike generator according to measured V_{iEEG}. Θ was therefore defined as the set of all iEEG contacts involved at the peak of the average iEEG spike, they were visually identified by an expert epileptologist (EK). $min_{j\in\Theta}(D_{ij})$ refers to the minimum distance between the contact i and the closest contact j found within the reference set Θ. This minimum distance was set to zero when this contact i belonged to the reference set Θ. $V_{MEG,i}^{2}$ denotes the energy of the electric potential estimated at the contact i. SD actually measures a combination of spatial spread around the true extent Θ and localization error when comparing V_{MEG} with V_{iEEG} results. SD was estimated for each of the five time samples around the peak of the average MEG spike, and the average SD value was reported. The fourth metric consisted in a ratio of spurious activity (RSA), assessing the amount of activity localized with MEG, distant from the presumed iEEG focus. To do so, we defined as distant iEEG contacts all contacts located at least 10 mm away from any contact of the reference set Θ. *RSA* was then computed as the ratio of the energy V_{MEG}^{2} estimated on distant contacts versus the energy V_{MEG}^{2} estimated on all contacts. RSA (in %) was estimated for each of the five time samples around the peak of the average MEG spike, and the average RSA value was reported.

RESULTS

We will first report detailed MEG/iEEG correlation for each patient using cMEM source localization. We chose cMEM to illustrate in detail every patient since cMEM showed overall among the best localization performance, as discussed in the last section of this article and as suggested in our previous studies [Chowdhury et al., 2013; Heers et al., 2016]. All source localization results were represented as the average over all epileptic spike localizations at the main peak of the spikes. The absolute value of the estimated current density map along the cortical surface was thresholded above the level of background activity using Otsu's method [Otsu, 1979]. Quantitative comparison between the estimated V_{MEG} and measured V_{iEEG} potentials for all source localization methods is then described (Table I).

Patient #1 had a very active right frontotemporal interictal focus on scalp EEG, with maximal involvement of electrodes F8, F10, T4, T10. Epileptic spikes over the same topography were also identified in MEG signals Figure 2a. MRI (3T) did not reveal any abnormalities. iEEG investigation was planned with a hypothesis of an underlying occult focal cortical dysplasia (FCD) in the right orbitofrontal area. Nine iEEG electrodes were inserted (Fig. 2b), confirming an almost continuous spiking activity in the superficial contacts of the right orbitofrontal electrode. Twenty-five epileptic spikes were marked in MEG and five highly reproducible and large amplitude epileptic spikes were marked in iEEG recordings. At the peak of the spike, the average of all MEG sources obtained using

[2]Anatomist software: http://brainvisa.info/doc/axon/en/help/aboutAnatomist.html

TABLE I. Comparison between source localization methods

	CMEM	MEM	IID	COH
(a) Corr values				
Patient 1	**0.71***	0.60*	0.27	0.53* ($\lambda_1 = 0.0000$, $\lambda_2 = 0.0052$)
Patient 2	**0.14**	**0.14**	0.11	0.03 ($\lambda_1 = 0.0000$, $\lambda_2 = 0.0474$)
Patient 3	**0.47***	0.33*	0.02	0.12 ($\lambda_1 = 0.0028$, $\lambda_2 = 0.0027$)
Patient 4	0.16	0.23	**0.38***	**0.38*** ($\lambda_1 = 0.0063$, $\lambda_2 = 0.0000$)
Patient 5	**0.39***	0.33	0.19	0.19 ($\lambda_1 = 0.0054$, $\lambda_2 = 0.0032$)
(b) D_{min} values (in mm)				
Patient 1	7.00	**0.00**	33.8	**0.00** ($\lambda_1 = 0.0000$, $\lambda_2 = 0.0052$)
Patient 2	**3.50**	**3.50**	20.4	**3.50** ($\lambda_1 = 0.0000$, $\lambda_2 = 0.0474$)
Patient 3	**7.00**	**7.00**	9.25	**7.00** ($\lambda_1 = 0.0028$, $\lambda_2 = 0.0027$)
Patient 4	**48.3**	**48.3**	73.3	73.3 ($\lambda_1 = 0.0063$, $\lambda_2 = 0.0000$)
Patient 5	**3.50**	11.9	14.0	14.0 ($\lambda_1 = 0.0054$, $\lambda_2 = 0.0032$)
(c) SD values (in mm)				
Patient 1	**10.6**	15.8	22.3	16.6 ($\lambda_1 = 0.0000$, $\lambda_2 = 0.0052$)
Patient 2	**19.2**	22.6	26.3	22.8 ($\lambda_1 = 0.0000$, $\lambda_2 = 0.0474$)
Patient 3	20.1	23.8	23.9	**18.3** ($\lambda_1 = 0.0028$, $\lambda_2 = 0.0027$)
Patient 4	30.5	30.6	**23.7**	**23.7** ($\lambda_1 = 0.0063$, $\lambda_2 = 0.0000$)
Patient 5	11.7	**10.1**	17.6	17.6 ($\lambda_1 = 0.0054$, $\lambda_2 = 0.0032$)
(d) RSA values (in %)				
Patient 1	**15.6**	28.6	31.9	20.9 ($\lambda_1 = 0.0000$, $\lambda_2 = 0.0052$)
Patient 2	**53.6**	67.6	79.0	57.3 ($\lambda_1 = 0.0000$, $\lambda_2 = 0.0474$)
Patient 3	**9.9**	15.6	23.9	15.7 ($\lambda_1 = 0.0028$, $\lambda_2 = 0.0027$)
Patient 4	80.7	86.7	**61.0**	**61.0** ($\lambda_1 = 0.0063$, $\lambda_2 = 0.0000$)
Patient 5	11.8	**10.1**	17.6	17.6 ($\lambda_1 = 0.0054$, $\lambda_2 = 0.0032$)

For each patient and for each source localization method, *Corr*, D_{min}, SD, and RSA quantitative comparison metrics between estimated V_{MEG} and recorded V_{iEEG} potentials are reported. The metric exhibiting the best performance for each patient is highlighted using bold font. We also tested whether Pearson's spatial correlation (*Corr*) was significantly non-null. Significant results at $p < 0.0025$ are indicated with a * ($p < 0.05/20 = 0.0025$, Bonferroni correction for 4 methods and 5 time samples). For COH, the ReML estimates of the hyperparameters associated to the minimum norm prior λ1 and to the spatial smoothness prior λ2 are indicated.

cMEM were found highly concordant with iEEG results, involving clearly a right orbitofrontal generator (Fig. 2c,d). The estimation of V_{MEG} potentials from cMEM sources was highly concordant with recorded V_{iEEG} potentials, involving mainly more superficial contacts of the right orbitofrontal electrode (contacts ROF6-9). Note that within this right orbitofrontal generator, V_{MEG} involved only one additional iEEG contact not seen in V_{iEEG} (ROF10), which is in agreement with cMEM accuracy to recover the spatial extent of the underlying generator. We also found a secondary cMEM source located in the right temporal lobe that projected with V_{MEG} on the more mesial contacts of the right amygdala electrode (contacts RA1–8). Because of its small amplitude, we may have missed such a source by analysing MEG signals only. It is very interesting to see that this secondary temporal source was highly reproducible across all epileptic spikes (small standard deviation) and concordant with iEEG recordings over the same contacts (RA1–8).

Patient #2 had also a very active right frontotemporal focus on scalp EEG, with concordant MEG epileptic spikes (Fig. 3a). A suspected right orbitofrontal FCD was seen on MRI. iEEG investigation with eight electrodes (Fig. 3b) was further guided by results of MEG sources, within the suspected MRI lesion. During iEEG, almost continuous spiking activity was seen in the superficial contacts of the right orbitofrontal electrode (contacts ROF8–12). Eight epileptic spikes were marked in MEG and 35 in iEEG recordings. Good spatial concordance between cMEM sources, estimated V_{MEG} potentials and recorded V_{iEEG} were found within the lateral right orbitofrontal region, where the FCD was suspected (Fig. 3). However, cMEM also showed a secondary right frontal pole source, that projected on RPF electrode in estimated V_{MEG} potentials (contacts RPF8–13). This secondary source was not seen in recorded V_{iEEG} potentials and could thus be considered as spurious. Moreover, V_{iEEG} time courses showed that the spiking activity started in the most superficial contacts of ROF electrode before propagating to the deepest contacts (ROF2–3) in few milliseconds (Fig. 3f). V_{MEG} potentials estimated using cMEM sources showed a slight involvement of these deepest ROF contacts (Fig. 3e) but not of sufficient amplitude to be detected from the level of background activity.

Patient #3 had multifocal scalp EEG findings including bursts of diffuse sharp and slow waves maximum in frontal areas, bilateral posterior quadrant slow waves bursts, rare left posterior temporoparietal epileptic spikes, and

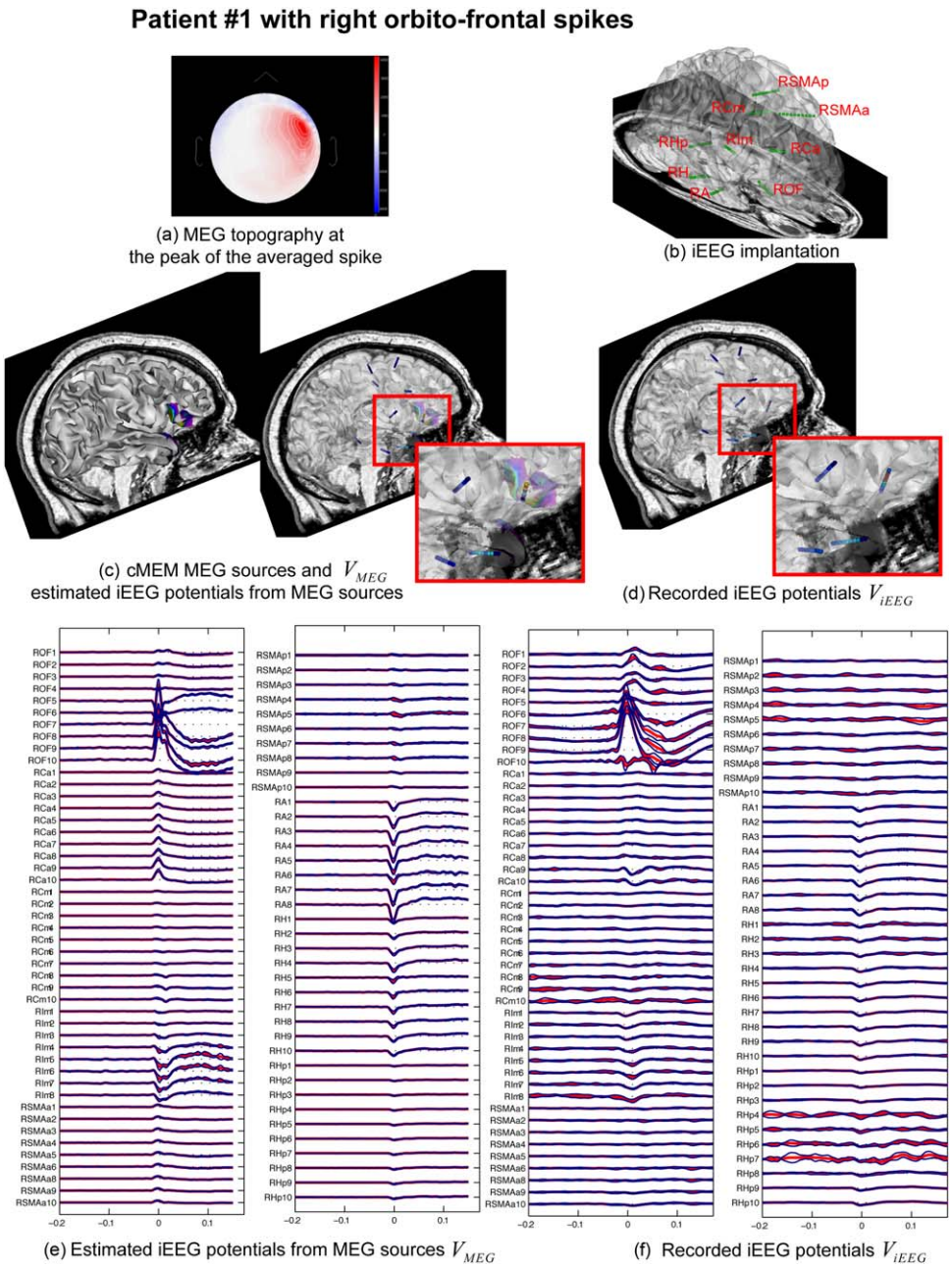

Figure 2.

MEG/iEEG correlation for Patient #1 with right orbitofrontal epileptic spikes. (**a**) MEG topography at the peak of the averaged epileptic spike. (**b**) iEEG implantation overview where each iEEG contact is represented in 3D as a green sphere (the cortical surface used for MEG source localization is shown with transparency). The label of each iEEG electrode is indicated: R: right, OF: orbito-frontal, A: amygdala, H: hippocampus, Hp: hippocampus posterior, Ca: anterior cingulate, Cm: mid cingulate, Im: mid insula, SMAa: anterior supplementary motor area, SMAp: posterior supplementary motor area. Electrodes contacts are labeled from 1 to 15, with 1 as the deepest contact in each electrode. Source localization were performed for every single epileptic spike and subsequently averaged. (**c**) cMEM source localization results and corresponding V_{MEG} potentials are presenting at the peak of the averaged epileptic spike. The absolute value of current density estimated using cMEM is shown as a colour texture over the cortical surface, thresholded above the level of background activity [Otsu, 1979], while the absolute value of V_{MEG} potentials is shown as a color texture over each electrode contact. (**d**) The absolute value of recorded iEEG potentials V_{iEEG} at the peak of the average epileptic spike is presented as a colour texture over each electrode contact. (**e**) Time courses of V_{MEG} potentials estimated over all iEEG contacts obtained for all epileptic spikes (average time course in red, $\pm$ standard deviation in blue). (**f**) Time courses of V_{iEEG} potentials recorded over all iEEG contacts for all epileptic spikes (average time course in red, $\pm$ standard deviation in blue). Here we observe an excellent spatial concordance between cMEM sources, estimated V_{MEG} potentials and recorded V_{iEEG} involving mainly a lateral right orbitofrontal generator. A secondary right temporal source involving the deepest contacts of RA electrodes was also found with V_{MEG} and confirmed with V_{iEEG}. [Color figure can be viewed in the online issue, which is available at wileyonlinelibrary.com.]

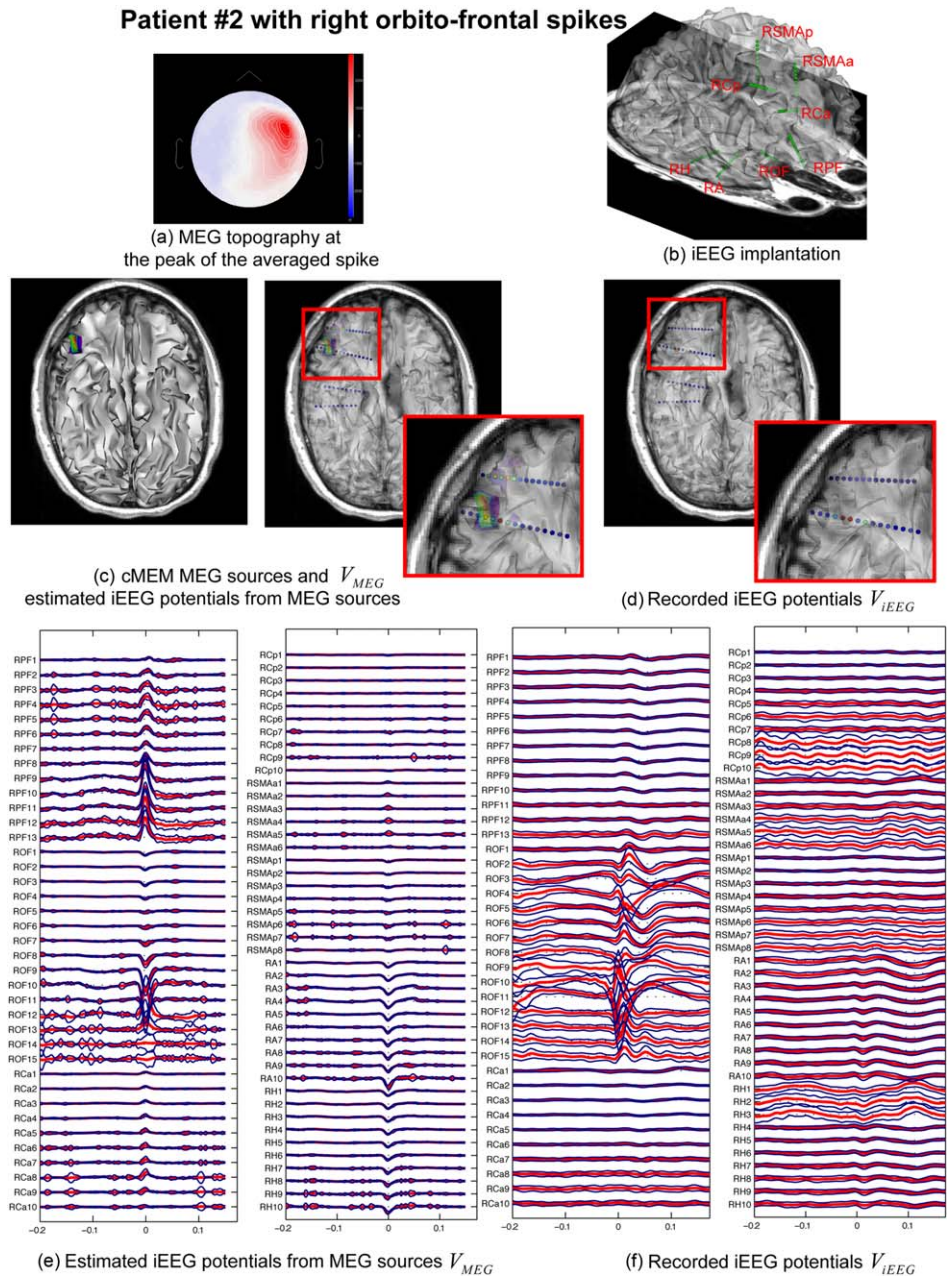

Figure 3.

MEG/iEEG correlation for Patient #2 with right orbitofrontal epileptic spikes. Overall organization as in Figure 2. Additional iEEG labels: PF: frontal pole, Cp: posterior cingulate. Here we observe an excellent spatial concordance between cMEM sources, estimated V_{MEG} potentials and recorded V_{iEEG} involving mainly a lateral right orbitofrontal generator (contacts ROF8-ROF12), while cMEM identified a secondary frontal source that projected on RPF superficial contacts. This secondary source was not seen in V_{iEEG} and could thus be considered as spurious. V_{iEEG} showed a propagation of the activity to the deepest ROF contacts. The involvement of these deepest contacts was barely seen in V_{MEG}, with very low amplitude. [Color figure can be viewed in the online issue, which is available at wileyonlinelibrary.com.]

rare bursts of low-amplitude fast activity in the right mid frontocentral region. MEG also showed different types of epileptic spikes: over the right anterior mesial frontal areas (Fig. 4a), over the left parietal area and bursts of slow waves with a bilateral distribution. Despite multifocal neurophysiology findings, a suspicious FCD at the right

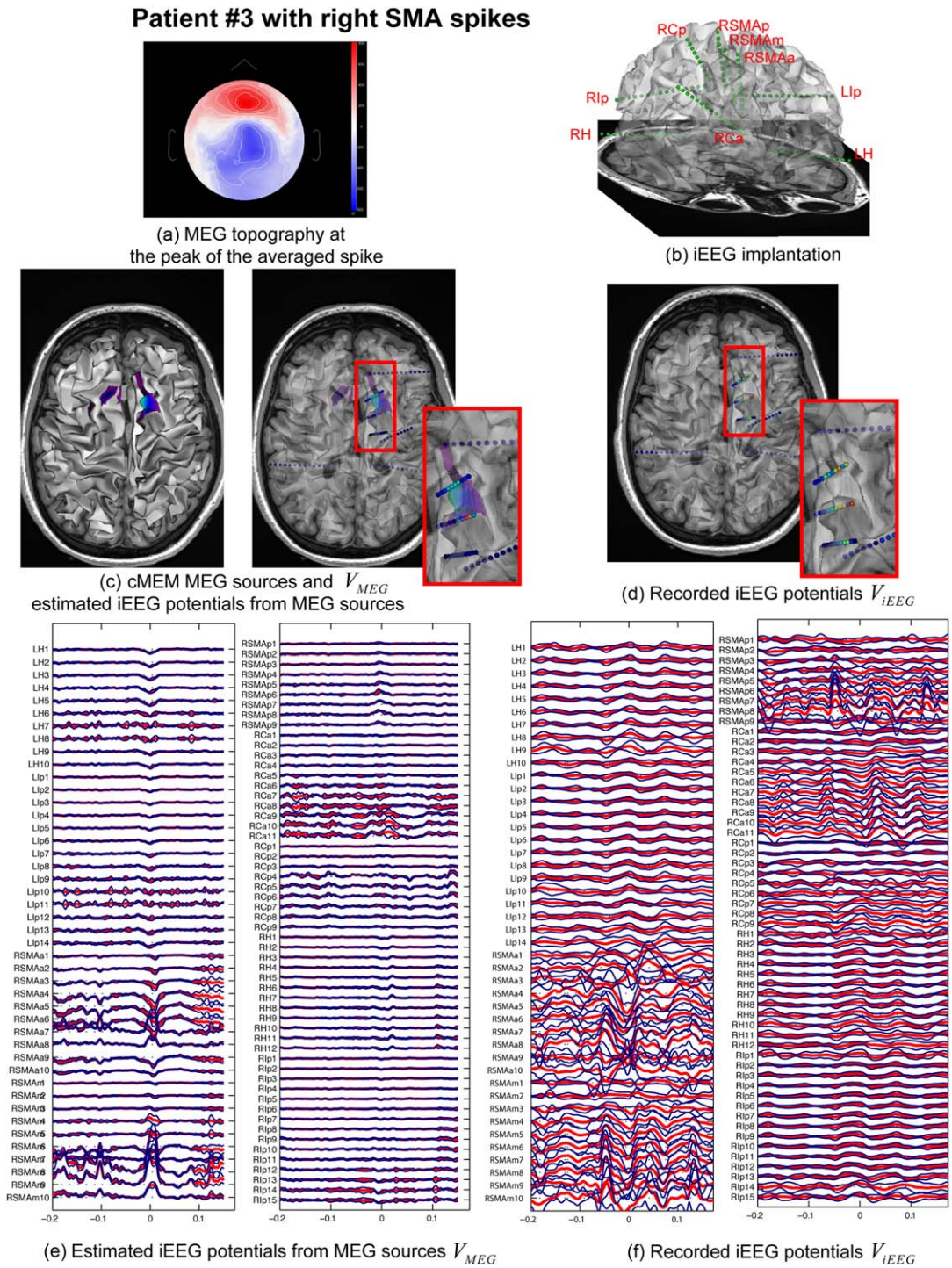

Figure 4.

MEG/iEEG correlation for Patient #3 with right supplementary motor area epileptic spikes. Overall organization as in Figure 2. Additional iEEG labels: L: left, SMAm: mid supplementary motor area, Ip: posterior insula. Here we observe a good spatial concordance between cMEM sources, estimated V_{MEG} potentials and recorded V_{iEEG} involving mainly a right SMA generator. Good concordance between V_{MEG} and V_{iEEG} was observed in RSMAa and RSMAm electrodes, whereas the secondary involvement of RSMAp on V_{iEEG} could not be retrieved from cMEM sources and estimated V_{MEG} potentials. [Color figure can be viewed in the online issue, which is available at wileyonlinelibrary.com.]

supplementary motor area/cingulate gyrus was identified in the MRI, and decision for an extensive iEEG investigation (9 electrodes) was taken, covering asymmetrically both hemispheres (Fig. 4b). iEEG targeting took into account information from MEG source localization for this patient. iEEG showed frequent sharp-waves and spike-waves involving multiple mid and superficial contacts of the anterior-SMA, mid-SMA, and posterior-SMA electrodes, indicating a widespread generator involving the right SMA. Note that there were also iEEG sharp waves in the superficial contacts of the left posterior temporal/inferior parietal electrode, in agreement with MEG spikes sources, but no ictal activities were recorded from this localization (results not shown). Only epileptic spikes likely to involve the right SMA were thus considered for MEG/iEEG correlation (6 epileptic spikes were marked in MEG and 6 in iEEG). We found good spatial concordance between cMEM sources, estimated V_{MEG} potentials and recorded V_{iEEG} involving mainly right SMA generators (Fig. 4), in the anterior and middle right SMA electrodes (contacts RSMAa3–8 and RSMAm4–10, Fig. 4e,f). V_{iEEG} showed a secondary involvement of the posterior SMA (contacts RSMAp5–8) that was not retrieved by cMEM sources. cMEM sources also localized a small source in the left frontal region, involving more likely dipoles with similar orientation as the main SMA source. Whereas such a source was probably spurious, no iEEG recording could further validate this statement as this area was not covered by iEEG implantation. Note that the epileptic spikes identified in iEEG were showing more variability than in the two previous cases, with large standard deviations (Fig. 4f), which further indicates the complexity of the underlying epileptic discharges for this patient.

Patient #4 has epilepsy associated with right hemisphere hemimegalencephaly in the context of hypomelanosis of Ito confirmed by biopsy. Scalp EEG recording showed two types of discharges: right frontotemporal epileptic spikes and bifrontal spike-waves or polyspike activity with right predominance. MEG also showed right frontal epileptic spikes (Fig. 5a). Despite the diffuse structural abnormality that predominated in the posterior quadrant region, neurophysiology abnormalities suggested a rather anterior predominance. Thus, the patient had nine implanted iEEG electrodes covering a widespread area in the right hemisphere (Fig. 5b). iEEG revealed an interictal focus on the superficial and intermediate contacts of the orbitofrontal electrode (contacts ROF12–15), that propagated rapidly to the deepest contacts of right orbitofrontal and right anterior insula electrodes (contacts ROF1–7, RIa1–3). Twelve epileptic spikes were marked in MEG and 28 in iEEG. Note that large standard deviation observed on V_{iEEG} time courses suggest large variability among these 28 iEEG spikes (Fig. 5f). At the peak of the epileptic spike, cMEM sources were found mainly along the right perisylvian region (Fig. 5c), resulting in estimated V_{MEG} potentials involving mainly more superficial contacts of the right anterior and posterior insula electrodes (contacts RIa9–15 and RIp10–15). No spatial concordance was found between V_{MEG} and V_{iEEG} at the peak of the epileptic spike. However, one can clearly see that the main right perisylvian cMEM source was located in brain regions not covered by iEEG electrodes (Fig. 5c), surrounded mainly by RIa and RIp electrodes, but also by RSMAp and RCm. In this context, we had no means to infer whether this main cMEM source was real or spurious. cMEM analysis of the ascending slope of the spike identified an early generator that projected in V_{MEG} over mid and superficial contacts of the right orbitofrontal electrode (contacts ROF4–15), in agreement with iEEG findings even though the main deep OF generator was not found from MEG sources.

Patient 5 had no unequivocal epileptiform discharges in scalp EEG, and many seizures were recorded in telemetry without a clear onset identified. Considered an EEG-negative patient, he underwent a MEG recording, where very low-amplitude repetitive epileptic spikes were seen throughout the examination over the inferior right frontal region (Fig. 6a). MEG source localization of these very low-amplitude spikes showed a very focal and clear source, which coincided with an area that was suspected for FCD on MRI, in the posterior aspects of the right inferior frontal region (Fig. 6c). iEEG investigation with seven electrodes (Fig. 6b) placed over the right hemisphere was guided by results of MEG sources, with electrodes inserted in the inferior and in the superior aspects of the source/lesion (RLi and RLs electrodes in Fig. 6b). During iEEG, there was a continuous spiking activity seen in the deepest contacts of these two electrodes, more so in the electrode located inferiorly (RLi). Interictal and ictal discharges were seen very focally with phase reversal at RLi2 contact. Sixty-one epileptic spikes were marked in MEG and compared with 41 epileptic spikes marked in iEEG. Excellent spatial concordance between cMEM sources, estimated V_{MEG} potentials and recorded V_{iEEG} was found within the lesion, involving maximally RLi2 contact for iEEG (referential montage) and RLi3 contact for MEG (Fig. 6c,d). cMEM source maps were extremely clean, showing no distant secondary sources at the time of the spike, suggesting that most of the parcels distant from the lesion were *switched off* during cMEM estimation. Comparing the resulting V_{MEG} and V_{iEEG} traces, we observed a good concordance within RLi electrode, involving very similar contacts for MEG (RLi2–6) and iEEG (RL2–4) (Fig. 6e,f). MEG-estimated potentials were also involving some more superficial contacts (RLi6 notably) not seen in iEEG. In iEEG, we also observed a secondary involvment of RLs electrodes, showing propagated activity occurring around 15–20 ms after the first peak of the spike and involving mainly RLs1–3 contacts. We also reconstructed some activity from MEG sources on RLs1–6 contacts in V_{MEG}. However, MEG activity reconstructed on RLs was found synchronous with the main peak of the spike seen in RLi, suggesting more likely some spread from the main reconstructed source

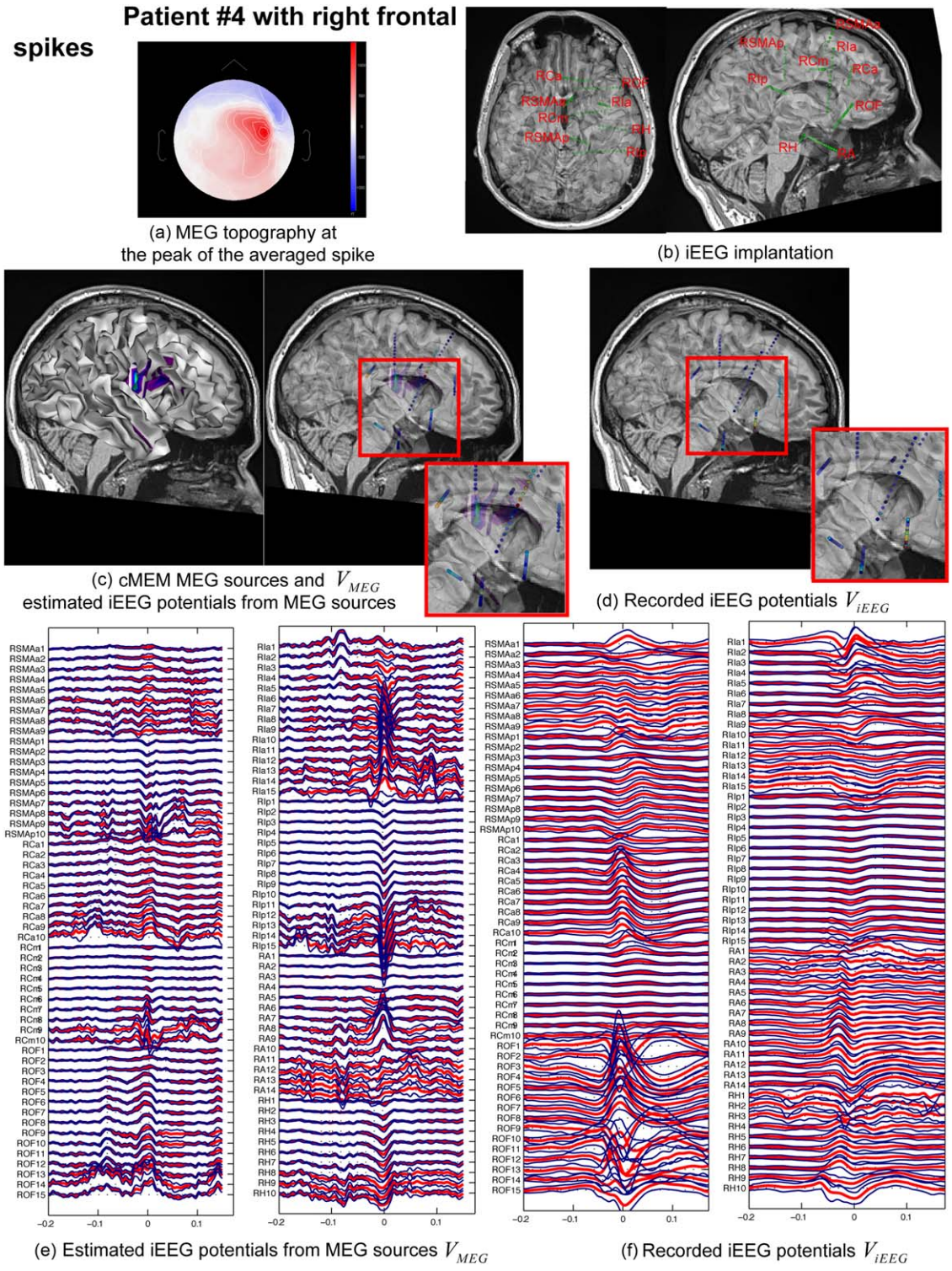

Figure 5.

MEG/iEEG correlation for Patient #4 with right frontal epileptic spikes. Overall organization as in Figure 2. Additional iEEG labels: Ia: anterior Insula. There was no clear spatial concordance between cMEM sources involving a right perisylvian source that projected mainly on RIa and RIp electrodes for V_{MEG}, as the main generator recorded using V_{iEEG} was obtained on the deepest contacts of ROF electrode (contacts ROF1–ROF7). Note that the time courses of recorded V_{iEEG} showed initial involvement of the most superficial contacts of ROF electrode (ROF12–ROF14), rapidly propagating to the deepest contacts. It could be considered that there is a slight MEG/iEEG concordance since estimated V_{MEG} potentials also showed a slight initial involvement of some mid and superficial ROF electrode contacts (ROF4–ROF15). No electrodes were implanted, where cMEM localized a right perisylvian source. [Color figure can be viewed in the online issue, which is available at wileyonlinelibrary.com.]

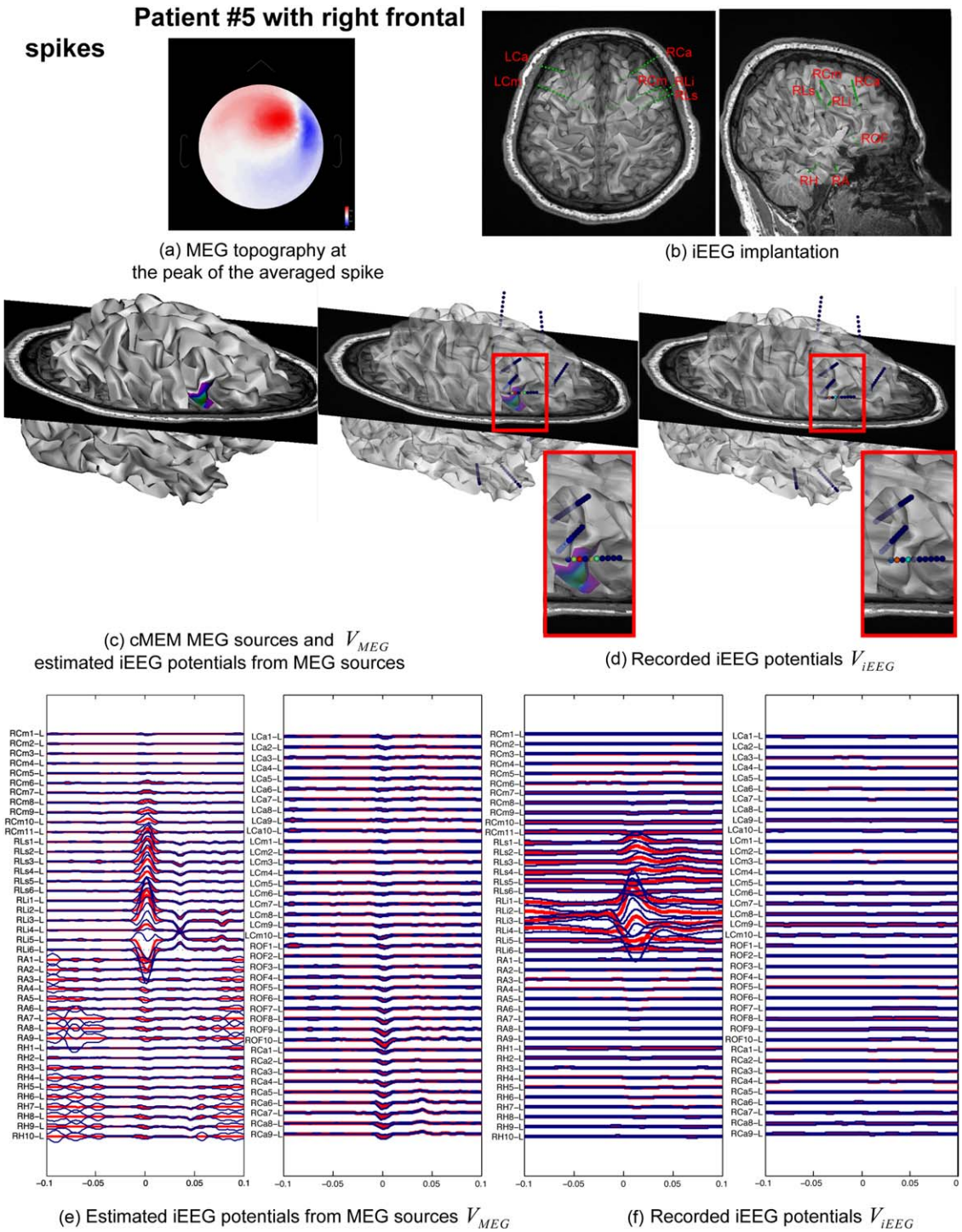

Figure 6.

MEG/iEEG correlation for Patient #5 with right frontal epileptic spikes. Overall organization as in Figure 2. Additional iEEG labels: Li and Ls, inferior and superior aspects of the lesion. Here, we observe an excellent spatial concordance between cMEM sources, estimated V_{MEG} potentials and recorded V_{iEEG}, within the suspected FCD lesion. The main reconstructed activity involved similar contacts on estimated V_{MEG} potentials (RLi2–6) and recorded V_{iEEG} potentials (RLi2–4). This is indeed a very focal generator that was propagating to the deepest contact of RLs electrodes (RLs1–3) few milliseconds after the main peak in iEEG. MEG reconstructed potentials V_{MEG} were spreading more than V_{iEEG} over RLi5–6 and RLs contacts, mainly because no other activity that the main generator was reconstructed using cMEM. This is an interesting example of a very focal generator localized accurately with MEG, whereas such a focal source was not able to generate visible epileptic spikes on scalp EEG. [Color figure can be viewed in the online issue, which is available at wileyonlinelibrary.com.]

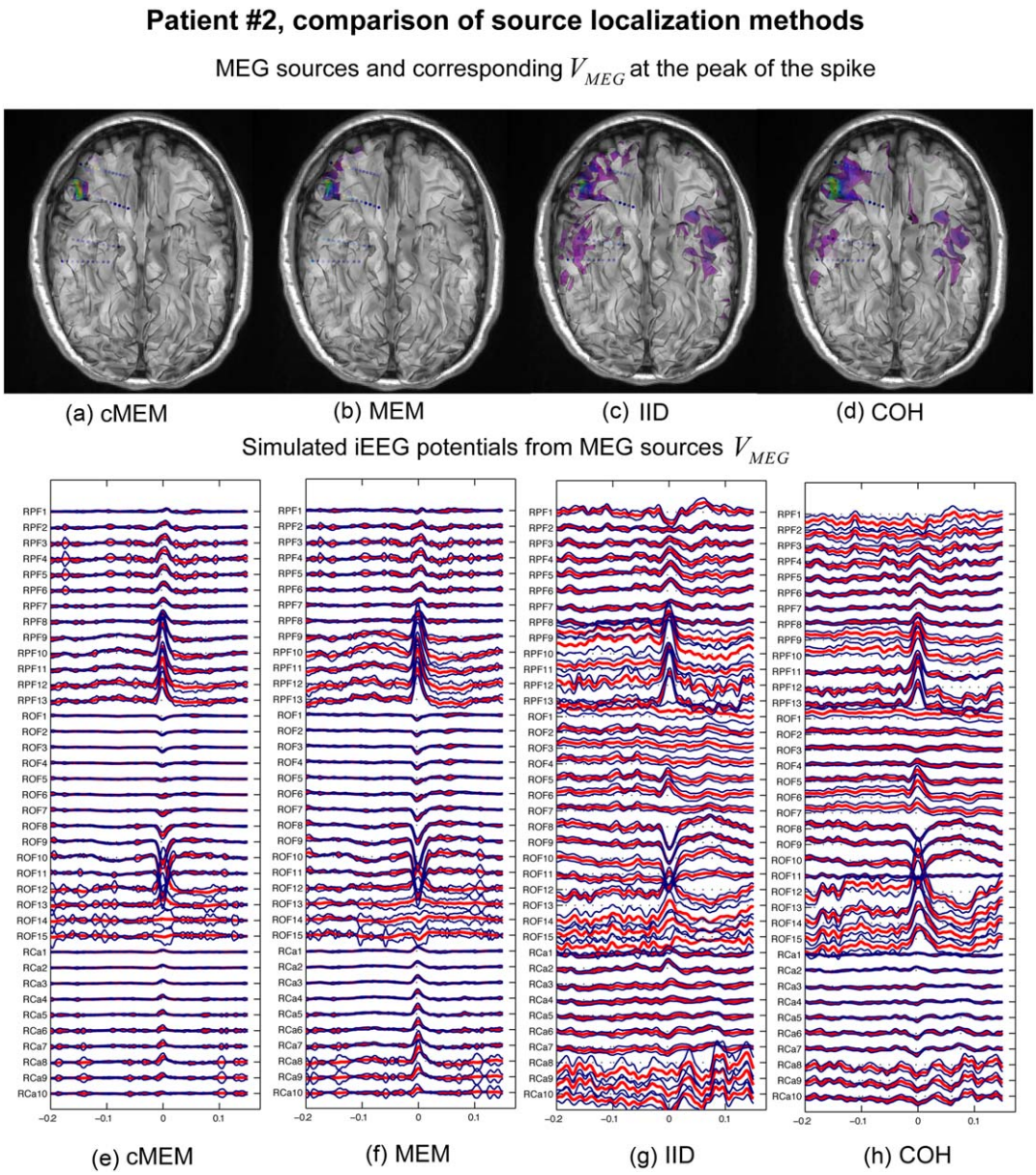

Figure 7.

Comparison between MEG source localization methods, illustrated in Patient #2 with right orbitofrontal epileptic spikes. For each source localization method, MEG source localization results and corresponding V_{MEG} potentials are presented at the peak of the averaged epileptic spike. The absolute value of current density estimated is shown as a color texture over the cortical surface, thresholded above the level of background activity [Otsu, 1979]. The absolute value of V_{MEG} potentials is shown as a color texture over each electrode contact: (**a**) cMEM sources, (**b**) MEM sources, (**c**) IID sources, and (**d**) COH sources. For each source localization method, time courses of V_{MEG} potentials estimated over iEEG contacts obtained for all epileptic spikes (average time course in red, $\pm$standard deviation in blue): (**e**) cMEM sources, (**f**) MEM sources, (**g**) IID sources, and (**h**) COH sources. V_{MEG} time courses are presented only on iEEG electrodes exhibiting most of the estimated activity (i.e., RPF, ROF, and RCa). These figures should be compared with iEEG recordings in Figure 3 (d) and (f). All four source localization methods found the main source located on the most superficial ROF electrode contacts. They also showed the same secondary spurious source that projected over RPF electrode. Overall source localizations obtained using IID and COH were noisier than MEM and cMEM, showing more extended spurious sources located far from the main generator. Fewer spurious sources were identified using both MEM and cMEM. [Color figure can be viewed in the online issue, which is available at wileyonlinelibrary.com.]

rather than a propagation pattern as seen in iEEG (Fig. 6c). Since reconstructed MEG activity around the main generator was more likely set to zero by cMEM, we could expect to observe some more distant interpolation when computing V_{MEG}. Indeed, MEG activity on the cortical surface located close to RLs electrode was more likely set to zero by cMEM, and therefore could not counteract the more distant influence from the reconstructed activity on the other side of the sulcus, explaining the spread of V_{MEG} signal on RLs electrode. Both MEG and iEEG findings are suggesting a very focal generator, explaining the reason why no clear epileptic spikes were seen on scalp EEG, and small ones were indeed observed in MEG. The patient underwent surgical resection, with confirmation of FCD IIb with balloon cells. The patient is seizure-free for three years after the surgery (surgery in November 2012).

Comparison between source localization methods: Although only cMEM results were presented so far, the same analyses were done using MEM, IID, and COH source localization methods. To summarize these results for each patient and for each source localization method, quantitative comparison results obtained using the four proposed metrics (*Corr*, D_{min}, *SD*, and *RSA*) are reported in Table I. For spatial correlation results (Corr), we also tested whether Pearson's correlation was significantly non-null. Results were considered as significant for *p*-values lower than 0.0025, i.e., $p < 0.05/20 = 0.0025$, taking into account Bonferroni correction for 4 methods and 5 time samples. Significant correlations were reported using a *, whereas methods showing the best performance for each source localization are reported using bold font in Table I.

Overall all proposed metric showed very consistent measurements among the 5 time samples chosen around the peak of the average MEG spike. cMEM showed the largest spatial correlation (Corr) values for Patients #1–3 and #5, whereas IID and COH showed the largest correlation for Patient #4. V_{iEEG}/V_{MEG} correlations were found significantly non null for 3/5 patients for cMEM, 2/5 patients for MEM and COH, and for 1/5 patient for IID. Minimum distances between contacts showing maximum activity in V_{iEEG} and V_{MEG} were found mainly for cMEM and MEM (Patients #1–3 and 5), as well as for COH (Patients #1–3), showing in most cases distances corresponding to maximum three consecutive contacts (i.e., $D_{min} = 7$ mm) or lower. Measurement of spatial spread around the true extent of the generator, using SD metric, was found most accurate for cMEM for Patients #1 and #2, for MEM for Patient #5 and for COH for Patients #3 and #4. These results suggest that these methods were able to recover accurately the true spatial extent of the underlying generator, whereas IID exhibited the worst SD results, suggesting an overestimation of the true spatial extent in most cases. cMEM and MEM also exhibited the smallest ratios of spurious activity (for Patients #1, #3, and #5), whereas IID and sometimes COH tended to exhibit more often some distant spurious activity. Overall our results are suggesting excellent performance of cMEM and MEM methods, with also very interesting properties of COH method, although with slightly less stability. The performance of IID was overall lower than the three other methods for most quantitative metrics. The proposed metrics are also showing that all methods exhibited the same spurious frontal source for Patient #2 (projected on RPF electrode in V_{MEG}), as illustrated in Figure 7 (cf. large RSA values, low *Corr* values). Quantitative comparison results for Patient #4 were overall biased, since no electrode was placed close to the main right perisylvian source localized in MEG by all methods. All methods failed in localizing the iEEG orbitofrontal deep generator.

In the last column of Table I, we indicated the ReML estimates of the two hyperparameters considered for COH model: $\lambda 1$ refers to the weight of the minimum norm prior and $\lambda 2$ refers to the weight of the spatial smoothness prior [Friston et al., 2002]. Interestingly, COH showed the best V_{iEEG}/V_{MEG} correlation for Patient #1, where ReML actually favoured the spatial smoothness prior. ReML also favoured the spatial smoothness prior for Patient #2, a mix of the two priors for Patient #3 and #5 and only the minimum norm prior for Patient #4.

A detailed illustration of the comparison of the four methods on Patient #2 is presented in Figure 7. All four source localization methods found the main source located on the more superficial contacts of ROF electrodes (Fig. 7) and also the same secondary spurious source that projected over RPF electrodes with V_{MEG}. Overall, source localizations obtained using IID and COH were noisier than MEM and cMEM results. Indeed, V_{MEG} time courses exhibited larger standard deviations for IID and COH than for MEM and cMEM, both at the peak of the epileptic spike and in the background (see RCa8–10, ROF12–15, RPF8–12 on Fig. 7g,h). These findings suggest that IID and COH were showing more spatially spread and also distant spurious sources, whereas fewer of those spurious sources were identified by MEM and cMEM. Whereas one could argue that, for patient #2, IID and COH exhibited a slight involvement of deeper ROF contacts (ROF5–6), without showing the propagation suggested by V_{iEEG} (Fig. 3f), they also overestimated the involvement of the more superficial ROF contacts (ROF13–15). On the other hand, the superficial ROF contacts found in V_{MEG} using MEM and cMEM (ROF9–11) were in excellent agreement with V_{iEEG} findings.

DISCUSSION

In this study, we proposed an original method allowing quantitative comparison between MEG sources and iEEG recordings from depth electrodes at the time of epileptic discharges. To do so, accurate localization of iEEG electrode contacts with the underlying anatomy used to model MEG sources was achieved using a postimplantation MRI together with iEEG electrodes in place. The void artefact

produced by the electrodes not only helps the clinical evaluation of recorded signals online (as we know exactly where we are recording from) but it also allows us to accurately localize each iEEG recording contact within the high resolution T1-weighted MRI. We assume that our iEEG/MRI registration strategy should result in a spatial accuracy of the order of 3 mm, as suggested by other similar approaches involving post-implantation CT or 2D X-ray radiographs [Dalal et al., 2008; Dykstra et al., 2012].

To further characterize the link between MEG sources and iEEG signals, we propose to convert MEG sources localized along the cortical surface into estimated iEEG potentials (V_{MEG}) by applying an iEEG forward model to current density distributions estimated from MEG data. A similar approach was proposed by Zhang et al. [2006] to convert sources estimated from scalp EEG (30 electrodes) into cortical electrical potentials to be compared with ECoG data. In this study, they considered a weighted MNE source localization on a simplified source space that did not take into account the underlying sulco-gyral anatomy to constrain the orientation of the dipolar sources. Following a similar strategy, Huiskamp and Agirre-Arrizubieta [2009] assessed whether the recorded ECoG epileptic spikes would correspond to the recorded MEG epileptic spikes. They estimated MEG signals from ECoG recordings by localizing first sources from ECoG data, followed by applying the MEG forward model to ECoG sources. Dalal et al. [2009] assessed MEG sensitivity to sources located between two iEEG contacts, applying the MEG forward model to each of these sources for different orientations. Here we proposed exactly the opposite approach to assess what part of MEG data could be accurately retrieved and validated by iEEG findings. Our method allowed us to demonstrate good correlations between estimated V_{MEG} potentials obtained from MEM and cMEM sources and recorded V_{iEEG} potentials for 4 out of 5 patients, while clearly exhibited the usual pitfalls of MEG source localization versus iEEG investigation, such as the lack of sensitivity of MEG sources to retrieve deeper generators. Note also that the same large amplitude spurious sources, as illustrated in Figure 7 for Patient #2, were found by all source localization methods evaluated, showing the limitation of most source localization methods. We also demonstrated that the main cMEM source found for Patient #4 could not be accurately retrieved and validated from the available iEEG data, since this brain region was not covered by the implantation. iEEG is a gold standard method to identify and confirm generators of epileptic activity [Chauvel et al., 1996] and it can validate MEG sources in implanted brain areas. Therefore, iEEG is only an incomplete gold standard as iEEG/MEG correlations is only valid within a close neighbourhood of each electrode contact. Correlations between MEG sources and invasive recordings has been mainly investigated using ECoG data [Agirre-Arrizubieta et al., 2009; de Gooijer-van de Groep et al., 2013; Fujiwara et al., 2012; Knowlton et al., 2006; Leijten et al., 2003; Mikuni et al., 1997; Minassian et al., 1999; Oishi et al., 2002; Tanaka et al., 2010], whereas some studies reported the comparison between MEG sources and iEEG recordings [Badier et al., 2015; Bouet et al., 2012; Gavaret et al., 2014; Jung et al., 2013; Schwartz et al., 2003], including our previous study reported in Heers et al. [2016]. Most of them consisted in qualitative description of the results, i.e., inference of sublobar accuracy between the two techniques. Whereas quantitative detection of the irritative and epileptogenic zone from iEEG data was provided in Badier et al. [2015], the correlation with MEG sources remained qualitative and at a sublobar level. In this study and as a continuation of our previous qualitative evaluation [Heers et al., 2016], we proposed a quantitative approach to compare iEEG/MEG data taking into account the limited spatial sampling of iEEG data. Our method seems quite promising to assess what part of MEG data could correspond to recorded iEEG data and therefore be accurately validated by this incomplete gold standard.

Understanding the relationship between scalp discharges (EEG or MEG) and iEEG recordings is a nontrivial task. Whereas simultaneous intracranial and scalp recordings could be considered [Dalal et al., 2009; Dubarry et al., 2014; Mikuni et al., 1997; Oishi et al., 2002], their clinical use remain quite limited because of technological and practical issues including infection risks. In our study, we compared MEG and iEEG epileptic spikes obtained from different acquisitions (3–15 months between MEG and iEEG investigations). Therefore, we paid specific attention to select, from iEEG traces, epileptic discharges involving some superficial contacts, characteristic of the epilepsy of each patient and reproducible. These iEEG discharges were then very likely involving the same generators as the epileptic discharges recorded during the MEG session.

Several iEEG studies, mainly in the field of neurosciences, proposed strategies to link iEEG recording with the underlying anatomy along the cortical surface to produce 3D images of iEEG analysis (e.g., gamma band response) at the individual or group level [David et al., 2011; Miller et al., 2007; Pei et al., 2011]. In these studies, the link between iEEG recordings and the cortical surface was obtained using local extrapolation kernels (e.g., spheres, Gaussian kernels) around each electrode contact. In this study, we rather wanted to use an interpolation scheme, from the cortical surface to iEEG electrodes, that was physically relevant. This is why we chose to use an iEEG forward model, taking explicitly into account the contribution of local dipolar sources of different orientations to iEEG measurements. Since we did not intend to solve the inverse problem of source localization from iEEG data, we used a simplified iEEG forward model assuming an infinite volume conductor characterized by a conductivity σ of 0.25 $S \cdot m^{-1}$. Cosandier-Rimélé et al. [2007] suggested that even such a simplified model could mimic almost perfectly real iEEG measurements in temporal lobe epilepsy.

Using finite-element models taking into account the actual size of the iEEG electrode contacts, von Ellenrieder et al. [2012] showed that the shape of the electrodes had almost no influence on local electrical potentials at a distance of 2 mm from the electrodes. Whereas the impact of the presence of an electrode on local electric potentials was first suggested as quite important especially on the borders of the electrodes [Church et al., 1985], subsequent modeling studies showed that the high-impedance thin layer generated by interaction between the electrode and local ions in the solution significantly reduced this local impact, within a neighbourhood of 2 mm around the electrode [Cheng et al., 1989; Somersalo et al., 1992; von Ellenrieder et al., 2012]. Consequently, we omitted to model the actual shape of every iEEG electrode contact and considered them as a point-size electrode contact for the estimation of the iEEG forward model. Although the dipolar model assumed by Eq. (4) does not hold when the distance between the source and the electrode is too small, we decided to prevent instabilities by limiting the source–electrode distance to minimum of 3 mm, while preserving the actual orientation of every dipolar source of the cortical surface (see Eq. (5)). This distance was chosen since it was larger than the 2 mm zone of influence reported by von Ellenrieder et al. [2012] and it also corresponded to the expected iEEG/MRI registration accuracy. Moreover, because of the inherent limits in spatial resolution of any source localization methods [Molins et al., 2008], the current density estimates obtained on every vertex are at best representing a local averaging of the underlying source density over few square millimeters. Therefore, we could hypothesize that every reconstructed source estimate should be located at least 3 mm away from any iEEG contact, what would justify that we are not dealing with very close interferences between current sources and iEEG electrodes contacts. In the few studies that reported source localization from ECoG data [Cho et al., 2011; Dumpelmann et al., 2009; Fuchs et al., 2007; Ramantani et al., 2013; Zhang et al., 2008], the ECoG forward model was generally estimated either using BEM or Finite Element Models. Several compartments were included: the inner skull surface only, the three standard head surfaces (inner skull, outer skull, and skin) or these three standard surfaces and the silastic ECoG pads. None of these studies modeled the impact of the electrode size. Whereas most of these studies considered electrical conductivity to be isotropic, von Ellenrieder et al. [2012] showed that modeling conductivity anisotropy within the white matter obtained from diffusion MRI had important impact on local electric potentials measured with iEEG. These possible improvements of the iEEG forward model, crucial to solve the iEEG inverse problem, will be considered for future investigations. However, we think that, in the context of this study, its overall impact on iEEG estimation from MEG sources through the application of the iEEG forward model should be minimal.

In addition to the evaluation of MEG/iEEG correlations, the proposed quantitative analysis provided also an ideal framework to compare source localization methods. Previous studies comparing different source localization methods when localizing epileptic activity using MEG [de Gooijer-van de Groep et al., 2013; Fujiwara et al., 2012] or EEG [Gavaret et al., 2006; Koessler et al., 2010; Michel et al., 2004] reported sublobar accuracy. In this study, we reported on five clinical cases, the comparison of two MEM-based source localization methods [Chowdhury et al., 2013] with two standard methods implemented within the Hierarchical Bayesian framework [Friston et al., 2002] in SPM8 software[3]: IID which is equivalent to a Minimum Norm estimate [Hämäläinen and Ilmoniemi, 1994] and COH which is a mix between a Minimum Norm estimate and a LORETA-like solution assuming spatial smoothness along the cortical surface [Pascual-Marqui et al., 1994]. The same methods were carefully evaluated using simulated MEG data mimicking the generation of epileptic spikes over different spatial extents ranging from 3 to 30 cm^2 in Chowdhury et al. [2013], and then validated on both EEG (56 electrodes) and MEG source localization of epileptic spikes on 15 patients with focal epilepsy [Heers et al., 2016]. Whereas a detailed qualitative evaluation assessing sublobar accuracy between EEG/MEG source localization and iEEG data was proposed in Heers et al. [2016], our present quantitative evaluation by estimating iEEG potentials from MEG sources V_{MEG} allowed us to reproduce similar findings, even if just a limited number of patients could be investigated with the present method, due to the availability of patients implanted with MR compatible electrodes. We notably considered four complementary comparison metrics similar to some proposed in Heers et al. [2016] to quantitatively compare V_{MEG} with V_{iEEG} for the four source localization methods investigated. Indeed, we showed that cMEM and to some extent MEM provided overall the most accurate results for MEG epileptic spike localization, by (i) recovering accurately the location and spatial extent of the underlying generators (cf Corr, D_{min}, and SD) and (ii) by avoiding the occurrence of distant spurious secondary sources (cf. RSA). Indeed, IID and COH were usually overestimating the spatial extent of the underlying generators, whereas cMEM was able to provide a more accurate contrast along actual the extent of the generator. Moreover, as opposed to IID and COH, MEM and cMEM clearly exhibited less secondary sources distant from the focus, likely to correspond to distant spurious activity. However, whereas we could partly quantify such behavior using *RSA* metric, these "possibly spurious" secondary sources were also rarely covered by iEEG implantation [Heers et al., 2016]. In this study, we could further confirm this property of MEM and cMEM, by measuring the standard deviation of

[3]SPM8 software: http://www.fil.ion.ucl.ac.uk/spm/software/spm8/

V_{MEG} potentials obtained over all epileptic spikes, either in the focus but also in iEEG contacts located far from the focus (Fig. 7). We observed that V_{MEG} exhibited less variability (smaller standard deviation) for MEM and cMEM than for COH and IID in the focus but also on contacts distant from the focus. The reason why V_{MEG} potentials showed little variability outside the focus is explained by the ability of MEM and cMEM methods to *switch off* some parcels during MEM regularization (Supporting Information Figure S1). Overall COH was also evaluated as a quite promising technique to recover the spatial extent of the genertors, in agreement with our previous studies [Chowdhury et al., 2013; Heers et al., 2016], even if it tends to exhibit more secondary "possibly" spurious distant sources. Even if promising, these results are still preliminary and further investigations involving more patients will be considered in future studies. Note that our proposed method to correlate scalp finding with iEEG is mainly dependent on the accuracy of the source localization method [Chowdhury et al., 2013; Grova et al., 2006], its application to scalp EEG data will be possible if we make sure to have sufficient spatial sampling and coverage of the head to allow accurate source localization [Brodbeck et al., 2011]. This issue will require further investigations that were out of the scope of this study. The implementation of MEM and cMEM methods evaluated in this study is now available within the Brain entropy in Space and Time (BeST) toolbox that we released as a plug-in in Brainstorm software[4]. Finally, besides providing an ideal framework to compare and evaluate source localization methods, our proposed methodology to estimate/predict iEEG potentials from MEG sources could offer a nice quantitative evaluation framework for different clinical applications. For instance, it could be considered to assist in the automatic optimization of iEEG electrodes implantation planning. We plan to combine our proposed strategy to another promising method recently proposed by Zelmann et al. [2015], which consists in improving the explored volume of interest by optimally guiding iEEG electrode implantation within a computer assisted neuronavigation environment. In this context, our method, combining simulated iEEG data and estimated V_{MEG} potentials from real MEG data, will allow predicting the recorded iEEG potentials for different configurations of implanted depth electrodes. Our method could be useful to analyse whether the spatial sampling of iEEG was sufficient (i.e., that regions not covered by iEEG implantation were not the focus).

CONCLUSION

We proposed a new method to perform quantitative comparison of MEG sources with iEEG recordings during epileptic activity, taking explicitly into account the sparse spatial sampling of iEEG investigation using implanted MRI-compatible depth electrodes. The method consists in converting MEG sources estimated along the cortical surface into estimated iEEG potentials, by applying an iEEG forward model. This method is particularly useful to clarify what part of scalp signals in MEG could be retrieved and validated by iEEG data. This method is also easily transferable to analyze scalp EEG data. This approach offered an ideal framework to compare different source localization methods, showing that MEM, and particularly cMEM, were able to accurately recover the spatial extent of the underlying generators of epileptic activity with good specificity.

[4]BeST Toolbox tutorial: http://neuroimage.usc.edu/brainstorm/Tutorials/TutBEst

ACKNOWLEDGMENT

The authors would like to thank Dr. François Dubeau, head of EEG Dept. of the Montreal Neurological Institute, for providing access to iEEG signals from our patients. The authors would like to also thank Dr. P. Perucca and Dr. T. Ferrari-Marinho for their help in iEEG data retrieval and interpretation.

REFERENCES

Agirre-Arrizubieta Z, Huiskamp GJ, Ferrier CH, van Huffelen AC, Leijten FS (2009): Interictal magnetoencephalography and the irritative zone in the electrocorticogram. Brain 132:3060–3071.

Amblard C, Lapalme E, Lina JM (2004): Biomagnetic source detection by maximum entropy and graphical models. IEEE Trans Biomed Eng 51:427–442.

An D, Fahoum F, Hall J, Olivier A, Gotman J, Dubeau F (2013): Electroencephalography/functional magnetic resonance imaging responses help predict surgical outcome in focal epilepsy. Epilepsia 54:2184–2194.

Badier JM, Bartolomei F, Chauvel P, Bénar CG, Gavaret M (2015): Magnetic source imaging in posterior cortex epilepsies. Brain Topogr 28:162–171.

Bénar CG, Grova C, Kobayashi E, Bagshaw AP, Aghakhani Y, Dubeau F, Gotman J (2006): EEG-fMRI of epileptic spikes: Concordance with EEG source localization and intracranial EEG. Neuroimage 30:1161–1170.

Birot G, Albera L, Wendling F, Merlet I (2011): Localization of extended brain sources from EEG/MEG: The ExSo-MUSIC approach. Neuroimage 56:102–113.

Bouet R, Jung J, Delpuech C, Ryvlin P, Isnard J, Guenot M, Bertrand O, Mauguiere F (2012): Towards source volume estimation of interictal spikes in focal epilepsy using magnetoencephalography. Neuroimage 59:3955–3966.

Brodbeck V, Spinelli L, Lascano AM, Wissmeier M, Vargas MI, Vulliemoz S, Pollo C, Schaller K, Michel CM, Seeck M (2011): Electroencephalographic source imaging: A prospective study of 152 operated epileptic patients. Brain 134:2887–2897.

Chang N, Gulrajani R, Gotman J (2005): Dipole localization using simulated intracerebral EEG. Clin Neurophysiol 116:2707–2716.

Chauvel P, Vignal JP, Biraben A, Badier JM, Scarabin JM (1996) Stereo-encephalography. Multimethodological Assessment of the Epileptic Forms. New York: Springer Verlag. p 80–108.

Cheng KS, Isaacson D, Newell JC, Gisser DG (1989): Electrode models for electric current computed tomography. IEEE Trans Biomed Eng 36:918–924.

Cho JH, Hong SB, Jung YJ, Kang HC, Kim HD, Suh M, Jung KY, Im CH (2011): Evaluation of algorithms for intracranial EEG (iEEG) source imaging of extended sources: Feasibility of using iEEG source imaging for localizing epileptogenic zones in secondary generalized epilepsy. Brain Topogr 24:91–104.

Chowdhury RA, Lina JM, Kobayashi E, Grova C (2013): MEG source localization of spatially extended generators of epileptic activity: Comparing entropic and hierarchical bayesian approaches. PLoS One 8:e55969

Church P, Leduc A, Beique RA (1985): Sensitivity analysis of depth EEG electrodes to dipolar electric sources. IEEE Trans Biomed Eng 32:554–560.

Collins DL, Neelin P, Peters TM, Evans AC (1994): Automatic 3D intersubject registration of MR volumetric data in standardized Talairach space. J Comput Assist Tomogr 18:192–205.

Cosandier-Rimélé D, Badier JM, Chauvel P, Wendling F (2007): A physiologically plausible spatio-temporal model for EEG signals recorded with intracerebral electrodes in human partial epilepsy. IEEE Trans Biomed Eng 54:380–388.

Cosandier-Rimélé D, Merlet I, Badier JM, Chauvel P, Wendling F (2008): The neuronal sources of EEG: Modeling of simultaneous scalp and intracerebral recordings in epilepsy. Neuroimage 42:135–146.

Dalal SS, Baillet S, Adam C, Ducorps A, Schwartz D, Jerbi K, Bertrand O, Garnero L, Martinerie J, Lachaux JP (2009): Simultaneous MEG and intracranial EEG recordings during attentive reading. Neuroimage 45:1289–1304.

Dalal SS, Edwards E, Kirsch HE, Barbaro NM, Knight RT, Nagarajan SS (2008): Localization of neurosurgically implanted electrodes via photograph-MRI-radiograph coregistration. J Neurosci Methods 174:106–115.

Dale A, Sereno M (1993): Improved localization of cortical activity by combining EEG and MEG with MRI surface reconstruction: A linear approach. J Cogn Neurosci 5:162–176.

Daunizeau J, Grova C, Marrelec G, Mattout J, Jbabdi S, Pelegrini-Issac M, Lina JM, Benali H (2007): Symmetrical event-related EEG/fMRI information fusion in a variational Bayesian framework. Neuroimage 36:69–87.

David O, Blauwblomme T, Job AS, Chabardes S, Hoffmann D, Minotti L, Kahane P (2011): Imaging the seizure onset zone with stereo-electroencephalography. Brain 134:2898–2911.

de Gooijer-van de Groep KL, Leijten FS, Ferrier CH, Huiskamp GJ (2013): Inverse modeling in magnetic source imaging: Comparison of MUSIC, SAM(g2), and sLORETA to interictal intracranial EEG. Hum Brain Mapp 34:2032–2044.

Ding L (2009): Reconstructing cortical current density by exploring sparseness in the transform domain. Phys Med Biol 54:2683–2697.

Dubarry AS, Badier JM, Trebuchon-Da Fonseca A, Gavaret M, Carron R, Bartolomei F, Liegeois-Chauvel C, Regis J, Chauvel P, Alario FX, Benar CG (2014): Simultaneous recording of MEG, EEG and intracerebral EEG during visual stimulation: From feasibility to single-trial analysis. Neuroimage 99:548–558.

Dumpelmann M, Fell J, Wellmer J, Urbach H, Elger CE (2009): 3D source localization derived from subdural strip and grid electrodes: A simulation study. Clin Neurophysiol 120:1061–1069.

Duncan JS (2010): Imaging in the surgical treatment of epilepsy. Nat Rev Neurol 6:537–550.

Dykstra AR, Chan AM, Quinn BT, Zepeda R, Keller CJ, Cormier J, Madsen JR, Eskandar EN, Cash SS (2012): Individualized localization and cortical surface-based registration of intracranial electrodes. Neuroimage 59:3563–3570.

Ebersole JS (1997): Defining epileptogenic foci: Past, present, future. J Clin Neurophysiol 14:470–483.

Friston KJ, Penny W, Phillips C, Kiebel S, Hinton G, Ashburner J (2002): Classical and Bayesian inference in neuroimaging: Theory. Neuroimage 16:465–483.

Fuchs M, Wagner M, Kastner J (2007): Development of volume conductor and source models to localize epileptic foci. J Clin Neurophysiol 24:101–119.

Fujiwara H, Greiner HM, Hemasilpin N, Lee KH, Holland-Bouley K, Arthur T, Morita D, Jain SV, Mangano FT, Degrauw T, Rose DF (2012): Ictal MEG onset source localization compared to intracranial EEG and outcome: Improved epilepsy presurgical evaluation in pediatrics. Epilepsy Res 99:214–224.

Gavaret M, Badier JM, Bartolomei F, Benar CG, Chauvel P (2014): MEG and EEG sensitivity in a case of medial occipital epilepsy. Brain Topogr 27:192–196.

Gavaret M, Badier JM, Marquis P, McGonigal A, Bartolomei F, Regis J, Chauvel P (2006): Electric source imaging in frontal lobe epilepsy. J Clin Neurophysiol 23:358–370.

Gevins A, Le J, Martin NK, Brickett P, Desmond J, Reutter B (1994): High resolution EEG: 124-channel recording, spatial deblurring and MRI integration methods. Electroencephalogr Clin Neurophysiol 90:337–358.

Goncalves SI, de Munck JC, Verbunt JP, Bijma F, Heethaar RM, Lopes da Silva F (2003): In vivo measurement of the brain and skull resistivities using an EIT-based method and realistic models for the head. IEEE Trans Biomed Eng 50: 754–767.

Gotman J (2008): Epileptic networks studied with EEG-fMRI. Epilepsia 49:42–51.

Gramfort A, Papadopoulo T, Olivi E, Clerc M (2011): Forward field computation with OpenMEEG. Comput Intell Neurosci 2011:923703

Grave de Peralta Menendez R, Gonzalez Andino SL, Morand S, Michel CM, Landis T (2000): Imaging the electrical activity of the brain: ELECTRA. Hum Brain Mapp 9:1–12.

Grova C, Daunizeau J, Kobayashi E, Bagshaw AP, Lina JM, Dubeau F, Gotman J (2008): Concordance between distributed EEG source localization and simultaneous EEG-fMRI studies of epileptic spikes. Neuroimage 39:755–774.

Grova C, Daunizeau J, Lina JM, Benar CG, Benali H, Gotman J (2006): Evaluation of EEG localization methods using realistic simulations of interictal spikes. Neuroimage 29:734–753.

Hamalainen M, Hari R, Ilmoniemi R, Knuutila J, Lounasmaa O (1993): Magneto-encephalography–theory, instrumentation, and applications to noninvasive studies of the working human brain. Rev Mod Phys 65:1–93.

Hämäläinen MS, Ilmoniemi RJ (1994): Interpreting magnetic fields of the brain: Minimum norm estimates. Med Biol Eng Comput 32:35–42.

Harrison LM, Penny W, Ashburner J, Trujillo-Barreto N, Friston KJ (2007): Diffusion-based spatial priors for imaging. Neuroimage 38:677–695.

He B, Zhang X, Lian J, Sasaki H, Wu D, Towle VL (2002): Boundary element method-based cortical potential imaging of somatosensory evoked potentials using subjects' magnetic resonance images. Neuroimage 16:564–576.

Heers M, Chowdhury RA, Hedrich T, Dubeau F, Hall JA, Lina JM, Grova C, Kobayashi E (2016): Localization accuracy of distributed inverse solutions for electric and magnetic source

imaging of interictal epileptic discharges in patients with focal epilepsy. Brain Topogr. 29(1):162–181.
Heers M, Hedrich T, An D, Dubeau F, Gotman J, Grova C, Kobayashi E (2014): Spatial correlation of hemodynamic changes related to interictal epileptic discharges with electric and magnetic source imaging. Hum Brain Mapp 35:4396–4414.
Hillebrand A, Barnes GR (2011): Practical constraints on estimation of source extent with MEG beamformers. Neuroimage 54: 2732–2740.
Huiskamp G, Agirre-Arrizubieta Z (2009): Interictal ECoG spikes as reflected in MEG. Conf Proc IEEE Eng Med Biol Soc 2009: 1930–1933.
Huiskamp G, Agirre-Arrizubieta Z, Leijten F (2010): Regional differences in the sensitivity of MEG for interictal spikes in epilepsy. Brain Topogr 23:159–164.
Ishii R, Canuet L, Ochi A, Xiang J, Imai K, Chan D, Iwase M, Takeda M, Snead OC3, Otsubo H (2008): Spatially filtered magnetoencephalography compared with electrocorticography to identify intrinsically epileptogenic focal cortical dysplasia. Epilepsy Res 81:228–232.
Juhasz C, Chugani HT (2003): Imaging the epileptic brain with positron emission tomography. Neuroimaging Clin N Am 13: 705–716, viii.
Jung J, Bouet R, Delpuech C, Ryvlin P, Isnard J, Guenot M, Bertrand O, Hammers A, Mauguiere F (2013): The value of magnetoencephalography for seizure-onset zone localization in magnetic resonance imaging-negative partial epilepsy. Brain 136:3176–3186.
Kim S, Mountz JM (2011): SPECT imaging of epilepsy: An overview and comparison with F-18 FDG PET. Int J Mol Imaging 2011:813028
Knake S, Halgren E, Shiraishi H, Hara K, Hamer HM, Grant PE, Carr VA, Foxe D, Camposano S, Busa E, Witzel T, Hamalainen MS, Ahlfors SP, Bromfield EB, Black PM, Bourgeois BF, Cole AJ, Cosgrove GR, Dworetzky BA, Madsen JR, Larsson PG, Schomer DL, Thiele EA, Dale AM, Rosen BR, Stufflebeam SM (2006): The value of multichannel MEG and EEG in the presurgical evaluation of 70 epilepsy patients. Epilepsy Res 69:80–86.
Knowlton RC, Elgavish R, Howell J, Blount J, Burneo JG, Faught E, Kankirawatana P, Riley K, Morawetz R, Worthington J, Kuzniecky RI (2006): Magnetic source imaging versus intracranial electroencephalogram in epilepsy surgery: A prospective study. Ann Neurol 59:835–842.
Knowlton RC, Elgavish RA, Bartolucci A, Ojha B, Limdi N, Blount J, Burneo JG, Ver Hoef L, Paige L, Faught E, Kankirawatana P, Riley K, Kuzniecky R (2008): Functional imaging: II. Prediction of epilepsy surgery outcome. Ann Neurol 64:35–41.
Knowlton RC, Laxer KD, Aminoff MJ, Roberts TP, Wong ST, Rowley HA (1997): Magnetoencephalography in partial epilepsy: Clinical yield and localization accuracy. Ann Neurol 42:622–631.
Kobayashi K, Yoshinaga H, Ohtsuka Y, Gotman J (2005): Dipole modeling of epileptic spikes can be accurate or misleading. Epilepsia 46:397–408.
Koessler L, Benar C, Maillard L, Badier JM, Vignal JP, Bartolomei F, Chauvel P, Gavaret M (2010): Source localization of ictal epileptic activity investigated by high resolution EEG and validated by SEEG. Neuroimage 51:642–653.
Kwan P, Brodie MJ (2000): Early identification of refractory epilepsy. N Engl J Med 342:314–319.
Kybic J, Clerc M, Faugeras O, Keriven R, Papadopoulo T (2006): Generalized head models for MEG/EEG: Boundary element method beyond nested volumes. Phys Med Biol 51:1333–1346.
Lapalme E, Lina JM, Mattout J (2006): Data-driven parceling and entropic inference in MEG. Neuroimage 30:160–171.
Leijten FS, Huiskamp GJ, Hilgersom I, Van Huffelen AC (2003): High-resolution source imaging in mesiotemporal lobe epilepsy: A comparison between MEG and simultaneous EEG. J Clin Neurophysiol 20:227–238.
Lina JM, Chowdhury R, Lemay E, Kobayashi E, Grova C (2014): Wavelet-based localization of oscillatory sources from magnetoencephalography data. IEEE Trans Biomed Eng 61:2350–2364.
Mangin J, Frouin V, Bloch I, Régis J, López-Krahe J (1995): From 3D magnetic resonance images to structural representations of the cortex topography using topology preserving deformations. J Math Imaging Vis 5:297–318.
Mattout J, Pelegrini-Issac M, Garnero L, Benali H (2005): Multivariate source prelocalization (MSP): Use of functionally informed basis functions for better conditioning the MEG inverse problem. Neuroimage 26:356–373.
Merlet I, Gotman J (2001): Dipole modeling of scalp electroencephalogram epileptic discharges: Correlation with intracerebral fields. Clin Neurophysiol 112:414–430.
Michel CM, Murray MM, Lantz G, Gonzalez S, Spinelli L, Grave de Peralta R (2004): EEG source imaging. Clin Neurophysiol 115:2195–2222.
Mikuni N, Nagamine T, Ikeda A, Terada K, Taki W, Kimura J, Kikuchi H, Shibasaki H (1997): Simultaneous recording of epileptiform discharges by MEG and subdural electrodes in temporal lobe epilepsy. Neuroimage 5:298–306.
Miller KJ, Leuthardt EC, Schalk G, Rao RP, Anderson NR, Moran DW, Miller JW, Ojemann JG (2007): Spectral changes in cortical surface potentials during motor movement. J Neurosci 27: 2424–2432.
Minassian BA, Otsubo H, Weiss S, Elliott I, Rutka JT, Snead OC3 (1999): Magnetoencephalographic localization in pediatric epilepsy surgery: Comparison with invasive intracranial electroencephalography. Ann Neurol 46:627–633.
Molins A, Stufflebeam SM, Brown EN, Hamalainen MS (2008): Quantification of the benefit from integrating MEG and EEG data in minimum l2-norm estimation. Neuroimage 42:1069–1077.
Noachtar S, Remi J (2009): The role of EEG in epilepsy: A critical review. Epilepsy Behav 15:22–33.
Oishi M, Otsubo H, Kameyama S, Morota N, Masuda H, Kitayama M, Tanaka R (2002): Epileptic spikes: Magnetoencephalography versus simultaneous electrocorticography. Epilepsia 43:1390–1395.
Olivier A, Germano IM, Cukiert A, Peters T (1994): Frameless stereotaxy for surgery of the epilepsies: Preliminary experience. Technical note. J Neurosurg 81:629–633.
Otsu N (1979): A threshold selection method from gray-level histograms. IEEE Trans Syst Man Cybern 9:62–66.
Papanicolaou AC, Pataraia E, Billingsley-Marshall R, Castillo EM, Wheless JW, Swank P, Breier JI, Sarkari S, Simos PG (2005): Toward the substitution of invasive electroencephalography in epilepsy surgery. J Clin Neurophysiol 22:231–237.
Pascual-Marqui RD, Michel CM, Lehmann D (1994): Low resolution electromagnetic tomography: A new method for localizing electrical activity in the brain. Int J Psychophysiol 18:49–65.
Pataraia E, Simos PG, Castillo EM, Billingsley RL, Sarkari S, Wheless JW, Maggio V, Maggio W, Baumgartner JE, Swank PR, Breier JI, Papanicolaou AC (2004): Does magnetoencephalography add to scalp video-EEG as a diagnostic tool in epilepsy surgery? Neurology 62:943–948.

Pei X, Leuthardt EC, Gaona CM, Brunner P, Wolpaw JR, Schalk G (2011): Spatiotemporal dynamics of electrocorticographic high gamma activity during overt and covert word repetition. Neuroimage 54:2960–2972.

Ramantani G, Cosandier-Rimele D, Schulze-Bonhage A, Maillard L, Zentner J, Dumpelmann M (2013): Source reconstruction based on subdural EEG recordings adds to the presurgical evaluation in refractory frontal lobe epilepsy. Clin Neurophysiol 124:481–491.

Schwartz DP, Badier JM, Vignal JP, Toulouse P, Scarabin JM, Chauvel P (2003): Non-supervised spatio-temporal analysis of interictal magnetic spikes: Comparison with intracerebral recordings. Clin Neurophysiol 114:438–449.

Shigeto H, Morioka T, Hisada K, Nishio S, Ishibashi H, Kira D, Tobimatsu S, Kato M (2002): Feasibility and limitations of magnetoencephalographic detection of epileptic discharges: Simultaneous recording of magnetic fields and electrocorticography. Neurol Res 24:531–536.

Somersalo E, Cheney M, Isaacson D (1992): Existence and uniqueness for electrode models for electric current computed tomography. SIAM J Appl Math 52:1023–1040.

Stefan H, Schneider S, Feistel H, Pawlik G, Schuler P, Abraham-Fuchs K, Schlegel T, Neubauer U, Huk WJ (1992): Ictal and interictal activity in partial epilepsy recorded with multichannel magnetoelectroencephalography: Correlation of electroencephalography/electrocorticography, magnetic resonance imaging, single photon emission computed tomography, and positron emission tomography findings. Epilepsia 33:874–887.

Sutherling WW, Crandall PH, Cahan LD, Barth DS (1988): The magnetic field of epileptic spikes agrees with intracranial localizations in complex partial epilepsy. Neurology 38:778–786.

Sutherling WW, Mamelak AN, Thyerlei D, Maleeva T, Minazad Y, Philpott L, Lopez N (2008): Influence of magnetic source imaging for planning intracranial EEG in epilepsy. Neurology 71:990–996.

Tadel F, Baillet S, Mosher JC, Pantazis D, Leahy RM (2011): Brainstorm: A user-friendly application for MEG/EEG analysis. Comput Intell Neurosci 2011:879716

Tanaka N, Hamalainen MS, Ahlfors SP, Liu H, Madsen JR, Bourgeois BF, Lee JW, Dworetzky BA, Belliveau JW, Stufflebeam SM (2010): Propagation of epileptic spikes reconstructed from spatiotemporal magnetoencephalographic and electroencephalographic source analysis. Neuroimage 50: 217–222.

Tao JX, Baldwin M, Hawes-Ebersole S, Ebersole JS (2007): Cortical substrates of scalp EEG epileptiform discharges. J Clin Neurophysiol 24:96–100.

Theodore WH (1989): SPECT and PET in epilepsy. Lancet 1:502–503.

von Ellenrieder N, Beltrachini L, Muravchik CH (2012): Electrode and brain modeling in stereo-EEG. Clin Neurophysiol 123: 1745–1754.

von Ellenrieder N, Beltrachini L, Perucca P, Gotman J (2014): Size of cortical generators of epileptic interictal events and visibility on scalp EEG. Neuroimage 94:47–54.

Wennberg R, Cheyne D (2014): Reliability of MEG source imaging of anterior temporal spikes: Analysis of an intracranially characterized spike focus. Clin Neurophysiol 125:903–918.

Zelmann R, Beriault S, Marinho MM, Mok K, Hall JA, Guizard N, Haegelen C, Olivier A, Pike GB, Collins DL (2015): Improving recorded volume in mesial temporal lobe by optimizing stereotactic intracranial electrode implantation planning. Int J Comput Assist Radiol Surg 10:1599–1615.

Zhang Y, Ding L, van Drongelen W, Hecox K, Frim DM, He B (2006): A cortical potential imaging study from simultaneous extra- and intracranial electrical recordings by means of the finite element method. Neuroimage 31:1513–1524.

Zhang Y, van Drongelen W, Kohrman M, He B (2008): Three-dimensional brain current source reconstruction from intracranial ECoG recordings. Neuroimage 42:683–695.